FREEZE-THAW DURABILITY OF CONCRETES WITH INFILLING OF ETTRINGITE IN VOIDS

Final Report
For
MLR-94-9 - Phase 2

April 1997

Project Development Division

Iowa Department of Transportation

FREEZE-THAW DURABILITY OF CONCRETES WITH INFILLING OF ETTRINGITE IN VOIDS

Final Report
for
MLR-94-9 - Phase 2

By
Chengsheng Ouyang
Transportation Engineer Associate
515-239-1088

and

O. J. Lane
Testing Engineer
515-239-1237

FAX: 515-239-1092
Office of Materials
Project Development Division
Iowa Department of Transportation
Ames, Iowa 50010

April 1997

TECHNICAL REPORT TITLE PAGE

1. REPORT NO.	2. REPORT DATE
MLR-94-9, Phase 2	April 1997

3. TITLE AND SUBTITLE	4. TYPE OF REPORT & PERIOD COVERED
Freeze-Thaw Durability of Concretes With Infilling of Ettringite in Voids	Final report, Phase 2, 1-96 TO 4-97

5. AUTHOR(S)	6. PERFORMING ORGANIZATION ADDRESS
Chen Ouyang Transportation Engineer Assoc. O. J. Lane Testing Engineer	Iowa Department of Transportation Materials Department 800 Lincoln Way Ames, Iowa 50010

7. ACKNOWLEDGEMENT OF COOPERATING ORGANIZATIONS

—

8. ABSTRACT

Examination of field portland cement concrete cores, from Iowa pavements with premature deterioration, reveals extensive infilling of calcium sulfate aluminum (CSA) compound in their air voids. A previous study (Phase 1) has shown some evidence of the correlation between freeze-thaw durability of concretes and ettringite infilling. To further verify the previous observation, a more extensive experimental program was conducted in this Phase 2 study. A total of 101 concrete mixes were examined. Seven cements, six fly ashes, two water reducers and three coarse aggregates were used in the concrete mixes. Specimens were under moist curing for up to 223 days before being subjected to the freeze-thaw cycling. An environmental treatment consisting of three consecutive wet (70°F in distilled water)/dry (120°F in oven) cycles was applied to some specimens. Immediately prior to the freeze-thaw cycling, most specimens were examined by a low-vacuum scanning electron microscope (SEM) for their microstructure.

The results obtained further demonstrate the correlation between concrete freeze-thaw response and CSA compound infilling in the air voids. The extent of the infilling depends on the period of moist curing as well as the wet/dry treatment. The extent of the infilling also relates to materials used. Concrete mixes with extensive infilling are more vulnerable to the freeze-thaw attack. Based on the obtained results, material criteria on cements and fly ashes for mainline paving were proposed for minimizing potential infilling of CSA compound in concrete.

9. KEY WORDS	10. NO. OF PAGES
Portland cement concrete Pavement Ettringite Premature pavement deterioration Void infilling	48

TABLE OF CONTENTS

DISCLAIMER

1. INTRODUCTION

Premature deterioration of some pavements in Iowa has been reported for several years. After extensive research efforts, some potential causes which may be responsible for the deterioration include alkali-silica reaction[1], internal sulfate attack[2] and freeze-thaw attack[3][4].

Petrographic observations of cores from several concrete pavements in Iowa, using a low-vacuum scanning electron microscope, have found that many entrained air voids in matured and aged concrete are filled by calcium sulfate aluminate compound (CSA) which may be ettringite[2][5] and will be referred to as ettringite in this report.

The results obtained from Phase 1 of this study[3] have demonstrated some correlation between freeze-thaw durability and the ettringite infilling for concrete. Two possible mechanisms have been proposed to interpret the correlation. First, primary ettringite, which is formed only several hours after concrete mixing with water, normally redeposits in large voids through moisture migration. The infilling of ettringite in some air voids implies that these voids are somewhat water-accessible. Based on current understanding[6], only water-free and partially water-free air voids can be used to effectively release hydraulic and osmotic pressures occurring during freezing, and can function to protect concrete from freeze-thaw attack. When air voids are invaded by moisture, effectiveness of these water-accessible air voids might be already compromised before being filled by ettringite. In this sense, the infilling by ettringite may be somewhat of an indicator to illustrate the extent of water-accessible air voids. Secondly, the infilling may further increase the effective spacing factor and reduce effective air content. That leads to concrete which is more vulnerable to freeze-thaw attack.

Phase 2 is the extension of Phase 1 study[3]. Objectives of Phase 2 study include: (i) examination of different combinations of field materials for the extent of ettringite infilling as well as the freeze-thaw response; and (ii) verification of the two aforementioned mechanisms which correlate infilling of ettringite and freeze-thaw response.

2. MATERIALS, SPECIMENS AND TEST PROCEDURE

2.1 Materials

Seven cements and six fly ashes used in Iowa pavements were used in this study. Chemical properties of these cements and fly ashes are listed in Tables 1 and 2, respectively. These cements are ASTM C 150 Type I/II, except cement 2 which is Type IP. Fly ash 1 is ASTM C 618 Class F, whereas fly ashes 2-6 are Class C. Two water reducers, Prokrete N-3 and Conchem 25DP, were used. Fine aggregate from Cordova, Illinois, was used for all mixes. Three coarse aggregates were used. Mixes 1-35 (see Table 3) used medium grain dolomite from Shaffton Quarry. Mixes 36-66 (see Table 4) used fine grain dolomite from Sully Mine. Mixes 67-101 (see Table 5) used limestone from Fort Dodge Mine.

Iowa Department of Transportation Standard Mix C-4WR was used as the basis. Amounts of cement replaced by fly ash were 0%, 10% and 20%, respectively. As indicated in Tables 3, 4 and 5, a total of 101 mixes were used.

2.2 Specimens and Test Procedure

The test procedure used is described in Figure 1. Two 12" x 12" x 4" slabs were cast for each mix, and stored in a standard 100% humidity and 73°F moist room. Twenty-two

1 3/4" x 3 1/2" cores were drilled from the two slabs at the age of 28 days for each mix. These twenty-two cores were divided into two groups (eleven cores from each group), and cured under standard wet condition.

For the first group, after 62 days of moist curing, three cores from each mix were subjected to freeze-thaw cycling. Prior to the start of the cycling, an additional core was examined by a low-vacuum scanning electron microscope (SEM) to observe its microstructure for some selected mixes. Also, at the age of 62 days, the remaining seven cores were subjected to the wet/dry treatment, which consists of three consecutive wet (70°F in distilled water)/dry (120°F in oven) cycles. It is noted that 120°F is a possible real pavement temperature during summer in Iowa. After the treatment, four of these cores were cured in distilled water for another 56 days, whereas the other three were cured in 5% NaCl water. All these cores with the wet/dry treatment were subjected to the freeze-thaw cycling at the age of 132 days. Prior to the start of the cycling, SEM photomicrographs were taken using a core cured in distilled water for some selected mixes.

A similar procedure was applied to the second group, after the initial 152 days of moist curing (note: the first group underwent 62 days of moist curing). The test procedure described above is illustrated in Figure 1.

The freeze-thaw cycling consists of two hours of freezing in air (0°F) and 1½ hours of thawing in water (40°F). This is similar to ASTM C 666B. The cycling continues until the failure of the sample or after reaching 700 cycles.

Length changes of the cores tested were monitored after they were fabricated (at the age of 28 days). No significant expansion was observed until the start of the freeze-thaw cycling.

Selected cores are being tested for hardened air parameters by the linear traverse technique. That information will be available later.

3. IMAGE ANALYSIS

As previously mentioned, prior to the start of freeze-thaw cycling, most of the specimens were examined using a low-vacuum SEM to observe their microstructure. Image analysis was then applied to SEM photomicrographs to obtain quantitative information about voids and ettringite infilling. The procedure for the image analysis is described as follows:

A typical SEM photomicrograph is shown in Figure 2a. A Gaussian filter was applied to the original SEM photomicrograph for reducing noise (Figure 2b). After further using a threshholding process (Figure 2c), the original SEM photograph was converted to a binary image as shown in Figure 2d, where white areas indicate voids in the original photograph. These areas were quantitatively evaluated. Dividing the obtained value of the white areas by total area of matrix, which excludes area of aggregate particles, results in a void index which represents percentage of voids in the matrix. Since only voids not filled by ettringite were counted in this procedure, the obtained void index is referred to as the effective void index hereafter.

A corresponding sulfur map of the SEM photomicrograph shown in Figure 2a is presented in Figure 3a. This map was obtained by applying elemental mapping technique to

the original SEM photograph. By using a similar procedure of image analysis (Figures 3b and 3c), a binary image for sulfate compound was obtained in Figure 3d, where white areas illustrate the presence of sulfur. Since the sulfur detected in such a way is associated with the CSA compound, which is regarded as ettringite in this report, the white areas measured here indicate the extent of ettringite infilling. Dividing the white areas by total area of matrix leads to a sulfate infilling index which represents the percentage of ettringite infilling in the matrix. Note that the term of sulfate infilling index is equivalent to the ettringite infilling index in this report.

Each value of effective void index or sulfate infilling index reported in this study is the average of three to five measurements for most of the samples.

4. RESULTS AND DISCUSSION

4.1 Influence of Period of Moist Curing

Values of expansion after 300 freeze-thaw cycles are plotted against effective void index for specimens using Shaffton coarse aggregate in Figure 4. Values of the effective void index were measured using the image analysis technique previously discussed. The specimens weren't subjected to the wet/dry treatment, and were moist cured for 62 days and 152 days, respectively, prior to the start of the freeze-thaw cycling. While the expansion generally decreases with an increasing effective void index, the specimens cured for 152 days show much greater expansion than those cured for 62 days. Since the former is more saturated compared to the latter due to longer period of moist curing, one may assume that the former has a greater portion of voids filled by water than the latter. Therefore, the result

presented in Figure 4 may be regarded as evidence to support the first previously proposed mechanism. This mechanism indicates that penetration of water into air voids compromises their role to protect concrete from freeze-thaw attack.

4.2 Influence of the Wet/Dry Treatment

The wet/dry treatment used here consists of three consecutive wet (70°F in distilled water)/dry (120°F in oven) cycles. The temperature of 120°F is a possible pavement temperature during the summer in Iowa.

SEM photomicrographs and their corresponding sulfate maps for a mix using cement 5, fly ash 2, Conchem 25DP water reducer, and Shaffton aggregate are shown in Figures 5a, 5b, 5c and 5d. The specimens made with the same materials and mix proportion were subjected to different types of environmental treatments. Results of the specimens under continuously moist curing for 62 days and 152 days are presented in Figures 5a and 5c, respectively. On the other hand, results shown in Figures 5c and 5d are for the specimens subjected to the wet/dry treatment at ages of 132 and 223 days, respectively. These specimens were also subjected to additional 56 days of moist curing after the wet/dry treatment. The sulfate based elemental mapping shows that the specimens with the wet/dry treatment have much more ettringite infilling in their voids. This fact indicates that the wet/dry treatment accelerates redeposit of ettringite in air voids.

Some previous studies[7] indicate that approximately 180°F of temperature may be needed to accelerate redeposit of secondary ettringite in large voids in concrete. This is because primary ettringite, formed from the initial reaction between tricalcium aluminate

(C_3A) and sulfur trioxide (SO_3), will be decomposed when concrete is subjected to this temperature. However, the results presented here suggest that 120°F oven dry may be sufficient to speed up the redeposit of ettringite in large voids in concrete. This may be due to the fact that oven drying at 120°F, which can create some microcracks in concrete, would result in more air voids to be water-accessible. As a result, it is easier for ettringite to migrate more easily into these wet air voids.

The expansion after 300 freeze-thaw cycles is expressed as a function of the effective void index in Figure 6 for the specimens using Shaffton aggregate. The specimens were subjected to the wet/dry treatment after 62 days and 152 days of moist curing, respectively. It is seen that the larger the expansion, the smaller the effective void index. Since the two groups of specimens underwent another 56 days of moist curing before the start of the freeze-thaw cycling, their degree of saturation prior to the cycling might be similar. That is evidenced by their relationships between the expansion and the effective void index which can be approximately described by a single curve as shown in Figure 6. These results are in agreement with the first previously proposed mechanism.

4.3 Influence of Ettringite Infilling

The expansion after 300 freeze-thaw cycles for mixes using Shaffton aggregate and subjected to the wet/dry treatment is also plotted in Figure 7 against the sulfate (ettringite) infilling index which was measured by the image analysis technique as previously defined. The freeze-thaw cycling started at the age of 223 days. The expansion generally increases with an increasing of the sulfate infilling index. It is noted that, in addition to the sulfate

infilling index, the expansion is also a function of the effective void index as shown in Figure 6. Since values of the effective void index for this group of specimens are approximately in the range of 2.0% and 11.5%, this explains why the results presented in Figure 7 are quite scattered. Similar observation was also made for mixes using Sully aggregate as shown in Figure 8. The results shown in Figures 8 and 9 further verify the second previously proposed mechanism which indicates that infilling of ettringite may reduce effective air content and may lead to concrete more vulnerable to freeze-thaw attack.

4.4 Influence of Coarse Aggregate

In order to compare with Figure 7 where the result for the mixes with Shaffton aggregate is given, similar outcomes for the mixes using Sully and Fort Dodge aggregates are also plotted in Figures 9 and 10, respectively. While the mixes with fine grain dolomite from Sully and the mixes with limestone from Fort Dodge have a similar level of expansion after 300 freeze-thaw cycles, the mixes using medium grain dolomite from Shaffton (see Figure 7) generally show greater expansion.

4.5 Influence of Different Types of Water Reducers

Values of the sulfate infilling index for the mixes using the same materials except for Prokrete N-3 and Conchem 25DP water reducers, respectively, are compared in Figure 11a. While cement 5 and Shaffton aggregate were commonly used, the results for the mixes with fly ashes 2 and 3, respectively, are presented in Figure 11a. When fly ash 2 was used, the mixes with the two types of water reducers have almost identical values of the sulfate

infilling index. On the other hand, when fly ash 3 was used, the mix with Prokrete N-3 has much higher value of the infilling index compared to that with Conchem 25DP.

The results for the mixes using cement 7, fly ash 2 and Shaffton aggregate are also shown in Figure 11b. For this case, using either Prokrete N-3 and Conchem 25DP leads to almost identical values of the infilling index.

It is difficult to evaluate the influence of water reducers on sulfate infilling in concrete at this stage due to a limited amount of test data available. However, the result in Figure 11a seems to indicate the use of water reducers Prokrete N-3 and Conchem 25DP might have some effect on sulfate infilling in concrete pavements.

5. SULFATE INFILLING AND CEMENT CHEMISTRY

Since Type IP cement and Class F fly ash may have different hydration processes and rates compared to Type I/II cement and Class C fly ash, only the results for those mixes using Type I/II cements and Class C fly ashes are presented in this section. Additionally, the chemical component of C_3A is not available for Type IP cement or for Class F fly ash.

5.1 Effect of C_3A

The relationships between the sulfate infilling index, measured by the image analysis technique, and total tricalcium aluminate (C_3A) in the mixes are plotted in Figures 12 and 13 for the specimens with ages of 152 and 223 days, respectively. The specimens of 223 days were subjected to the wet/dry treatment, whereas those of 152 days were not. The total C_3A in the mix includes contributions from both cement and fly ash. According to Connell and

Higgins[8], the equivalent C_3A in Class C fly ash is approximately equal to 88.3% of the Al_2O_3 in fly ash. It is seen from Figures 12 and 13 that when the total C_3A is smaller than 8.5%, the value of the sulfate infilling index is relatively low. However, when the value of the total C_3A is greater than 8.5%, the sulfate infilling index might reach as high as 9%. It is noted that the value of 88.3% for equivalent C_3A in fly ash, suggested by Connell and Higgins[8], may be somewhat too high. Up to 10% of variation of this value will not change the observed trend of the sulfate infilling index in terms of the total C_3A as indicated in Figure 12.

The sulfate infilling index is also plotted against C_3A in cement in Figure 14 for the specimens with the wet/dry treatment at the age of 223 days, where C_3A in fly ash was not included. The result shows that the use of cement 7 with C_3A = 10.5% has high potential to result in more ettringite infilling in concrete. To reduce the potential of sulfate infilling in concrete, it may be appropriate to use cements with C_3A lower than 9.5% for mainline paving. This result also indicates that the use of Type II cements which have C_3A not greater than 8%, as proposed by Iowa Department of Transportation for primary roads, can significantly reduce ettringite infilling in concrete pavements.

5.2 Effect of Total Al_2O_3 in Mix

The sulfate infilling index against total alumina (Al_2O_3) in mix is shown in Figure 15, where the total Al_2O_3 in mix includes contributions from both cement and fly ash. When the total Al_2O_3 is greater than 7.2%, the possibility of severe ettringite infilling becomes high. Based on the level of the total Al_2O_3, the results shown in Figure 15 may be divided into two

groups: one without fly ash and the other with fly ash. For the group without fly ash, one out of ten mixes has the sulfate infilling index greater than 8%, whereas for the group with fly ashes, four out of 28 mixes have the sulfate infilling index higher than 8%. Since fly ashes generally have much higher content of Al_2O_3 compared to cements as shown in Tables 1 and 2, the use of Class C fly ash may increase potential ettringite infilling in concrete pavements.

In order to reduce the potential of ettringite infilling, it is proposed here that total Al_2O_3 in a mix should not exceed 7.2% for mainline paving in Iowa. This proposed criterion can eliminate those mixes with greater values of sulfate infilling index as indicated in Figure 15. This proposed criterion applies only to mixes using ASTM Type I/II cement and ASTM Class C fly ash, and total Al_2O_3 includes contributions from both cement and fly ash. The effect of this proposed criterion on total Al_2O_3 is illustrated in Figure 16. The maximum allowable amount of Al_2O_3 in fly ash generally deceases with an increasing amount of Al_2O_3 in cement. When a given cement with 4.5% of Al_2O_3 is used, the maximum allowable amount of Al_2O_3 in fly ash is 22.5% for 15% of fly ash replacement, and is 18% for 20% of fly ash replacement. For a given cement, if one would like to use a fly ash with higher content of Al_2O_3, he can slightly reduce the replacement level of fly ash. The potential impact of the proposed criterion on cements and Class C fly ash used in Iowa pavements is also demonstrated in Figure 16. As listed in Tables 1 and 2, the Al_2O_3 contents in cements used in Iowa pavements are in the range of 4.1% and 5.2%, whereas Class C fly ashes used have the Al_2O_3 contents between 15% and 21%. As shown as Figure 16, the proposed criterion imposes some limits on selections of cements and fly ashes for concrete mixes with

20% of fly ash replacement. However, these limits are very minor for mixes with 15% of fly ash replacement.

5.3 Effects of Total SO_3, $(Na_2O)_{eq.}$ and K_2O in Mix

The sulfate infilling index is plotted against the value of total SO_3 in mix, which is the sum of SO_3 in cement and fly ash, in Figure 17. Values of the total SO_3 in most of the concrete mixes tested are in the range of 2.6% and 3.2%. Within this range of SO_3, the corresponding values of the sulfate infilling index change approximately from 1% to 12%. For the concrete mixes tested, no rising trend of the ettringite infilling was observed when the total SO_3 in the mix increases.

The sulfate infilling index is also expressed as a function of total $(Na_2O)_{eq.}$ in mix in Figure 18. Values of the total $(Na_2O)_{eq.}$ were in the range of 0.4% and 0.8% for majority of the concrete mixes tested. Within this range, the influence of total $(Na_2O)_{eq.}$ on the sulfate infilling index is not obvious for the mixes tested.

The relationship between the sulfate infilling index and total K_2O in mix is demonstrated in Figure 19. The effect of K_2O (potassium oxide) is separated from Na_2O (sodium oxide) because the former is much more water-soluble than the latter. In ordinary portland cements, approximate 60%-90% of K_2O is water-soluble, whereas about 30%-50% of Na_2O is water-soluble. For specimens with K_2O in the range of 0.4% and 0.7%, the effect of total K_2O in mix is considered insignificant.

5.4 Effect of C_3A*SO_3 and C_3A*K_2O in Mix

To examine the coupling effect of C_3A and SO_3, the sulfate infilling index is plotted against the product of C_3A and SO_3 in mix in Figure 20. A greater value of C_3A*SO_3 generally leads to more ettringite infilling. This result was expected because ettringite is the reaction product between C_3A and SO_3 in concrete.

The relationship between the sulfate infilling index and the product of C_3A and K_2O is illustrated in Figures 21a, 21b and 21c for the specimens using Shaffton, Sully and Fort Dodge aggregates, respectively. The sulfate infilling index generally increases with an increasing value of C_3A*K_2O in mix. Concretes with greater values of C_3A*K_2O in mix have a higher potential to generate more ettringite infilling in their air voids. It seems that ettringite infilling not only depends on the C_3A amount in concrete mix, but also relates to the K_2O level.

6. MATERIAL CRITERION BASED ON SULFATE INFILLING

Freeze-thaw expansion may result in microcracks in concrete, which is usually accompanied by a loss of material strength. In order to quantitatively evaluate the strength loss due to freeze-thaw expansion, a strength ratio is introduced in this report. This strength ratio was obtained by dividing the compressive strength at a certain value of expansion with the compressive strength immediately prior to the start of the freeze-thaw cycling. The latter usually corresponds to zero expansion. The relationship between the strength ratio and the freeze-thaw expansion was experimentally measured in this study and is shown in Figure 22. Values of the strength ratio decrease with increasing expansion. As shown in Figure 22,

20% of strength loss (the strength ratio = 0.8) approximately corresponds to 0.1% of the freeze-thaw expansion, whereas 40% of the loss is related to 0.36% of the expansion. This relationship may be used as a criterion for evaluating freeze-thaw performance of concrete.

To use the above relationship to derive a material criterion, one should first determine an acceptable level of the strength ratio. As an example, if one regards that 30% of strength loss (the strength ratio = 0.7) is practically acceptable, the corresponding value of the expansion is equal to 0.2% as indicated in Figure 22. From the average relationship between the freeze-thaw expansion and the sulfate infilling index as shown in Figure 7, the value of sulfate infilling index = 6.5% can be determined when Shaffton aggregate was used. Then, according to Figure 14, cements with C_3A approximately lower than 10% should be used. In practice, it appears that cements with C_3A lower than 9.5% for mainline paving may be appropriate. The use of cements with C_3A content less than a certain value selected here may guarantee concrete with an acceptable level of sulfate (ettringite) infilling. This would not only be a benefit for the freeze-thaw response, as indicated in this study, but would also help to lower the potential for internal sulfate attack.

Material criteria for other selected acceptable levels of the strength ratio can also be similarly derived.

7. SUMMARY

Freeze-thaw response and sulfate infilling of concretes made by combinations of different field materials have been studied. Influences of many factors, such as period of moist curing, wet/dry treatment, cementitious chemistry and types of coarse aggregates, have

been experimentally studied. The following conclusions are obtained from this study:

1. A longer period of moist curing and the wet/dry treatment increases infilling of calcium sulfate aluminum (CSA) compound in the air voids. The temperature of 120°F, which may occur in Iowa pavements during summer, is sufficient to accelerate the redeposit of ettringite in large voids in the concrete.

2. The period of moist curing is the most important factor for freeze-thaw expansion. The specimens continuously soaked for 152 days, generally, had the greatest expansion.

3. For the specimens with a similar period of continuous moist curing, the expansion decreases with an increasing effective void index. The freeze-thaw expansion increases when more voids are filled by the CSA compound.

4. It is further confirmed that two previously proposed mechanisms may be responsible for the above observations. These include: (i) longer moist curing and the wet/dry treatment (which can create some microcracks in concrete) enable water to penetrate into some voids, which compromises these voids to protect concrete during freezing, and (ii) ettringite infilling reduces effective air content, which leads to concrete more vulnerable to freeze-thaw attack.

5. The amount of CSA compound significantly increases for mixes which used the cement with C_3A = 10.49%. When Type I/II cement and Class C fly ash are used, the possibility of ettringite infilling greatly increases when total Al_2O_3 content in a mix is greater than 7.2%.

6. To minimize potential ettringite infilling in concrete, two material criteria are proposed here for mainline paving: (i) the C_3A content in a Type I/II cement should not

exceed 9.5%; and (ii) when Type I/II cement and Class C fly ash are used, the total Al_2O_3 in a mix, which includes contributions from both cement and fly ash, should be smaller than 7.2%.

7. Concrete with greater values of C_3A*SO_3 or C_3A*K_2O generally has more ettringite infilling in its voids.

8. Generally, specimens made of the aggregate from Shaffton show the greatest freeze-thaw expansion, whereas specimens using the aggregate from Fort Dodge show the smallest expansion. It is still not clear why this happens. Further study is needed.

8. ACKNOWLEDGEMENTS

The authors thank the Cement and Concrete Section of the Iowa DOT Central Materials Laboratory for conducting the test. The authors also appreciate the input of C. Narotam, J. Bergren, V. Marks, J. Grove, T. Hanson and W. Dubberke from Iowa DOT. The discussion from members of Iowa DOT Materials Quality Task Group is acknowledged. Special thanks to J. Amenson and W. Straszheim of Iowa State University for their help in taking SEM photomicrographs and in conducting image analysis. Thanks are also due to A. Innis of LaFarge, Canada, Inc. for performing the linear traverse measurements of air parameters.

9. REFERENCES

1. Stark, D., "Investigation of Pavement Cracking in US 20 and I-35, Central Iowa," Construction Technology Laboratories, Inc., Skokie, September 1992.

2. Marks, V. J., and Dubberke, W. G., "A Different Perspective for Investigation of PCC Pavement Deterioration," Paper No. 960414, 75th Annual Meeting, Transportation Research Board, Washington, D.C., January 7-11, 1996.

3. Ouyang, C., and Lane, O. J., "Freeze-Thaw Durability of Concretes With and Without Class C Fly Ash," Final Report, MLR-9409, Phase 1, Iowa Department of Transportation, 1997.

4. Ouyang, C., and Lane, O. J., "Freeze-Thaw Durability of Concrete With and Without Class C Fly Ash," Materials for the New Millennium, Vol. 2, Edited by K. P. Chong, American Society of Civil Engineers, New York, 1996, pp. 939-948.

5. Schlorholtz, S., and Amenson, J., "Evaluation of Microcracking and Chemical Deterioration in Concrete Pavements," Final Report, Iowa DOT Project HR-358, Engineering Research Institute, Iowa State University, October, 1995.

6. Marchand, J., Sellevold, E. J. and Pigeon, M., "The Deicer Salt Scaling Deterioration of Concrete--an Overview," Durability of Concrete, ACI SP-145, American Concrete Institute, Detroit, 1995, pp. 1-46.

7. Day, R. L., "The Effect of Secondary Ettringite Formation on the Durability of Concrete: A Literature Analysis," Research and Development Bulletin RD108T, PCA R&D Serial No. 1929, Portland Cement Association, 1992 pp 113.

8. Connell and Higgins, Proceedings of the 9th International Conference on Alkali Aggregate Reaction in Concrete, Vol. 1, The Concrete Society, Slough, 1992, pp. 175-183.

TABLE TITLES

1. Chemical Properties of Cements Used
2. Chemical Properties of Fly Ashes Used
3. List of Mixes Using Shaffton Coarse Aggregate
4. List of Mixes Using Sully Coarse Aggregate
5. List of Mixes Using Fort Dodge Coarse Aggregate

Table 1 **Chemical Properties of Cements Used**

Cements	ASTM Type	C_3A (%)	SO_3 (%)	MgO (%)	Na_2O (%)	Al_2O_3 (%)	Fe_2O_3 (%)	SiO_2 (%)	CaO (%)	K_2O (%)
1	I/II	6.72	2.70	3.65	0.17	4.17	3.14	20.86	63.40	0.55
2	IP	-	3.13	1.90	0.12	9.95	3.62	26.33	51.63	0.45
3	I	7.52	3.77	4.31	0.06	4.54	3.07	19.12	61.89	1.15
4	I	9.69	2.87	2.75	0.10	5.11	3.10	19.66	62.94	0.69
5	I/II	7.63	2.87	2.85	0.13	4.76	3.49	20.03	63.15	0.62
6	I	9.33	2.78	2.68	0.16	4.67	2.37	20.76	61.14	0.48
7	I	10.49	3.07	2.93	0.06	5.18	2.29	20.91	63.00	0.62

Table 2 **Chemical Properties of Fly Ashes Used**

Fly Ashes	ASTM Class	SiO_2	Al_2O_3	Fe_2O_2	SO_3	CaO	MgO	Total $(Na_2O)_{eq.}$	Avail. $(Na_2O)_{eq.}$
1	F	50.73	32.88	2.38	0.77	5.70	1.20	0.93	0.33
2	C	33.35	15.92	6.93	3.44	29.10	6.53	1.79	1.14
3	C	36.52	20.37	5.65	1.74	25.36	4.74	1.44	0.88
4	C	34.66	16.05	6.81	2.53	28.50	6.24	1.63	1.01
5	C	33.83	17.63	6.19	2.92	28.33	5.57	2.40	1.45
6	C	35.51	20.28	5.68	2.53	27.03	4.84	1.56	0.51

Table 3 List of Mixes Using Shaffton Coarse Aggregate

Mix No.	Cement Source	Fly Ash		Water Reducer Source	Plastic Air Cont. (%)
		Source	(%)		
1	1	1 (F)	20	1	Not avail.
2	1	-	0	1	Not avail.
3	1	2	20	1	Not avail.
4	1	4	20	1	Not avail.
5	1	5	20	1	Not avail.
6	1	6	20	1	Not avail.
7	2 (IP)	1 (F)	10	1	Not avail.
8	2 (IP)	-	0	1	Not avail.
9	2 (IP)	2	10	1	Not avail.
10	2 (IP)	6	10	1	Not avail.
11	4	1 (F)	20	1	Not avail.
12	4	-	0	1	Not avail.
13	4	2	20	1	Not avail.
14	4	3	20	1	Not avail.
15	4	5	20	1	Not avail.
16	4	6	20	1	Not avail.
17	5	1 (F)	20	1	Not avail.
18	5	-	0	1	Not avail.
19	5	2	20	1	Not avail.
20	5	2	20	2	Not avail.
21	5	3	20	1	Not avail.
22	5	3	20	2	Not avail.
23	5	5	20	1	Not avail.
24	5	5	20	2	Not avail.
25	6	-	0	1	Not avail.
26	6	2	20	1	Not avail.
27	6	4	20	1	Not avail.
28	6	6	20	1	Not avail.
29	7	1 (F)	20	1	Not avail.
30	7	2	20	1	Not avail.
31	7	2	20	2	Not avail.
32	7	3	20	1	Not avail.
33	7	-	0	1	Not avail.
34	7	5	20	1	Not avail.
35	7	6	20	1	Not avail.

Table 4 List of Mixes Using Sully Coarse Aggregate

Mix No.	Cement Source	Fly Ash		Water Reducer Source	Plastic Air Cont. (%)
		Source	(%)		
36	1	1 (F)	20	1	5.6
37	1	-	0	1	6.9
38	1	2	20	1	6.8
39	1	4	20	1	6.6
40	1	5	20	1	6.4
41	1	6	20	1	6.3
42	2 (IP)	1 (F)	10	1	5.4
43	2 (IP)	-	0	1	6.6
44	2 (IP)	2	10	1	6.1
45	2 (IP)	6	10	1	6.3
46	3	1 (F)	20	1	5.5
47	3	3	20	1	6.0
48	3	-	0	1	6.2
49	3	5	20	1	5.9
50	4	1 (F)	20	1	5.5
51	4	-	0	1	6.0
52	4	2	20	1	5.7
53	4	3	20	1	5.5
54	4	5	20	1	5.5
55	4	6	20	1	5.7
56	5	1 (F)	20	1	5.6
57	5	-	0	1	6.0
58	5	2	20	1	6.3
59	5	3	20	1	6.2
60	5	5	20	1	5.8
61	7	1 (F)	20	1	5.5
62	7	2	20	1	6.1
63	7	3	20	1	5.9
64	7	-	0	1	6.0
65	7	5	20	1	6.4
66	7	6	20	1	6.4

Table 5 List of Mixes Using Fort Dodge Coarse Aggregate

Mix No.	Cement Source	Fly Ash		Water Reducer Source	Plastic Air Cont. (%)
		Source	(%)		
67	1	1 (F)	20	1	5.8
68	1	-	0	1	5.8
69	1	2	20	1	6.0
70	1	4	20	1	6.1
71	1	5	20	1	6.0
72	1	6	20	1	6.0
73	2 (IP)	1 (F)	10	1	5.8
74	2 (IP)	-	0	1	6.0
75	2 (IP)	2	10	1	6.1
76	2 (IP)	6	10	1	6.0
77	3	1 (F)	20	1	5.7
78	3	3	20	1	5.9
79	3	-	0	1	5.7
80	3	5	20	1	6.5
81	4	1 (F)	20	1	6.0
82	4	-	0	1	5.9
83	4	2	20	1	5.8
84	4	3	20	1	6.0
85	4	5	20	1	6.1
86	4	6	20	1	6.1
87	5	1 (F)	20	1	5.7
88	5	-	0	1	6.0
89	5	2	20	1	5.8
90	5	3	20	1	5.9
91	5	5	20	1	5.8
92	6	-	0	1	6.0
93	6	2	20	1	6.1
94	6	4	20	1	6.2
95	6	6	20	1	6.2
96	7	1 (F)	20	1	6.1
97	7	2	20	1	6.1
98	7	3	20	1	6.0
99	7	-	0	1	5.9
100	7	5	20	1	6.2
101	7	6	20	1	6.1

FIGURE CAPTIONS

1. Test Procedure for MLR-94-9, Phase 2 Study

2. Measurement of Effective Void Index by Image Analysis

3. Measurement of Sulfate Infilling Index by Image Analysis

4. Influence of Period of Moist Curing on Freeze-Thaw Response (Coarse Aggregate: Shaffton)

5. SEM Photomicrographs and Corresponding Sulfur Maps for the Mix Using Cement 5, Fly Ash 2, Conchem 25DP Water Reducer and Shaffton Aggregate

6. Influence of Effective Void Index on Freeze-Thaw Response (Coarse Aggregate: Shaffton)

7. Influence of Ettringite Infilling on Freeze-Thaw Response (Coarse Aggregate: Shaffton)

8. Influence of Ettringite Infilling on Freeze-Thaw Response (Coarse Aggregate: Sully)

9. Influence of Effective Void Index on Freeze-Thaw Response (Coarse Aggregate: Sully)

10. Influence of Effective Void Index on Freeze-Thaw Response (Coarse Aggregate: Fort Dodge)

11a Influence of Type of Water Reducer on Ettringite Infilling (Mixes Using Cement 5)

11b. Influence of Type of Water Reducer on Ettringite Infilling (Mixes Using Cement 7)

12. Effect of Total Tricalcium Aluminate in Mix on Ettringite Infilling (Specimens With Wet/Dry Treatment and Age of 223 Days)

13. Effect of Total Tricalcium Aluminate on Ettringite Infilling (Specimens Without Wet/Dry Treatment and Age of 152 Days)

14. Amounts of Sulfate Infilling for Different Types of Cements

15. Effect of Total Alumina in Mix on Ettringite Infilling

16. Illustration of Proposed Limit on Total Al_2O_3 in Mix

FIGURE CAPTIONS (Cont'd)

17. Effect of Total SO_3 in Mix on Ettringite Infilling

18. Effect of Total Equivalent Alkali on Ettringite Infilling

19. Effect of Total Potassium Alkali in Mix on Ettringite Infilling

20. Effect of C_3A*SO_3 in Mix on Ettringite Infilling

21a. Effect of C_3A*K_2O in Mix on Ettringite Infilling (Shaffton Coarse Aggregate)

21b. Effect of C_3A*K_2O in Mix on Ettringite Infilling (Sully Coarse Aggregate)

21c. Effect of C_3A*K_2O in Mix on Ettringite Infilling (Fort Dodge Coarse Aggregate)

22. Relationship Between Expansion and Strength Ratio

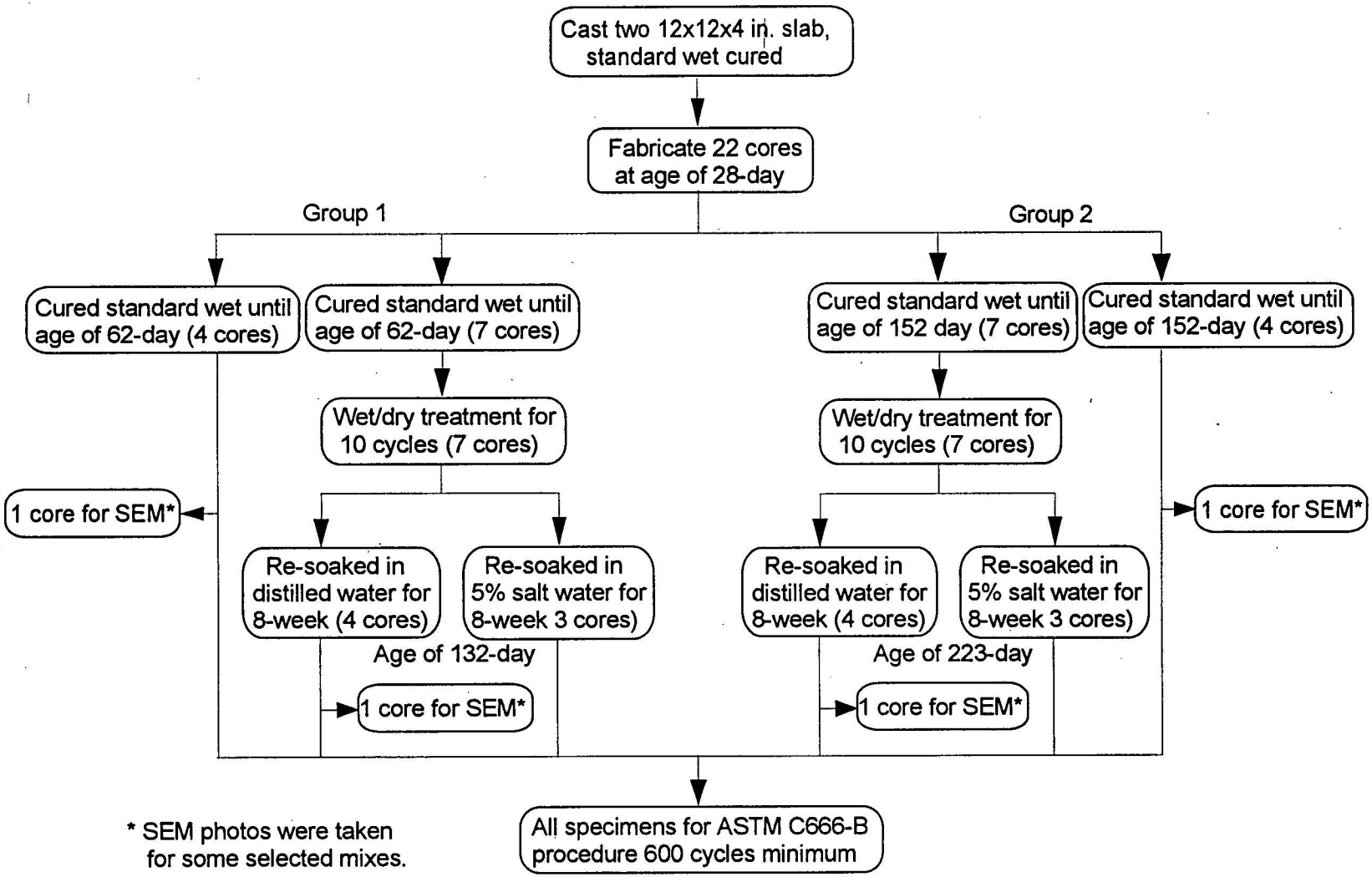

Fig. 1 Test procedure for MLR-94-9, Phase 2 study

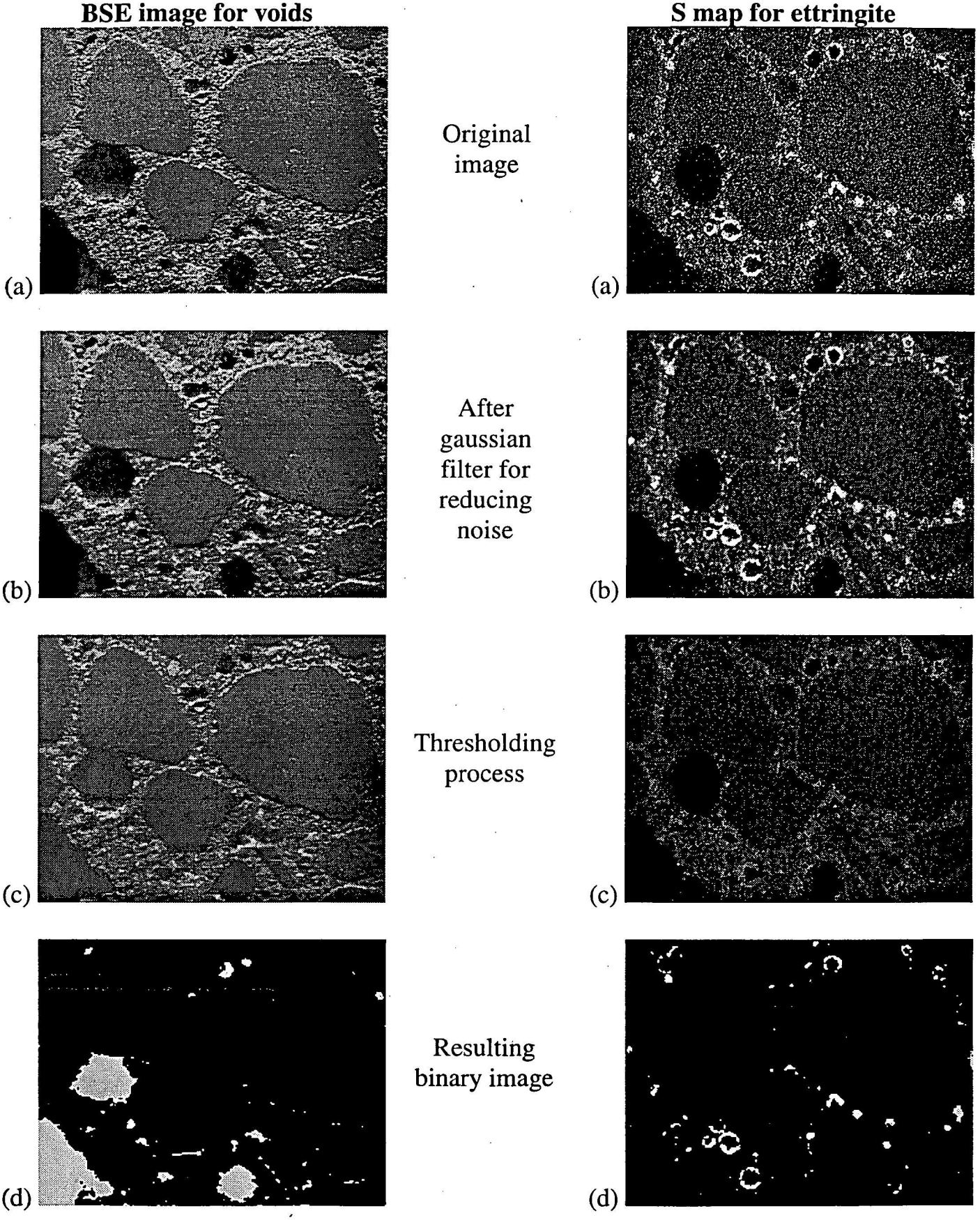

Fig.2 Measurement of effective void index by image analysis

Fig.3 Measurement of sulfate infilling index by image analysis

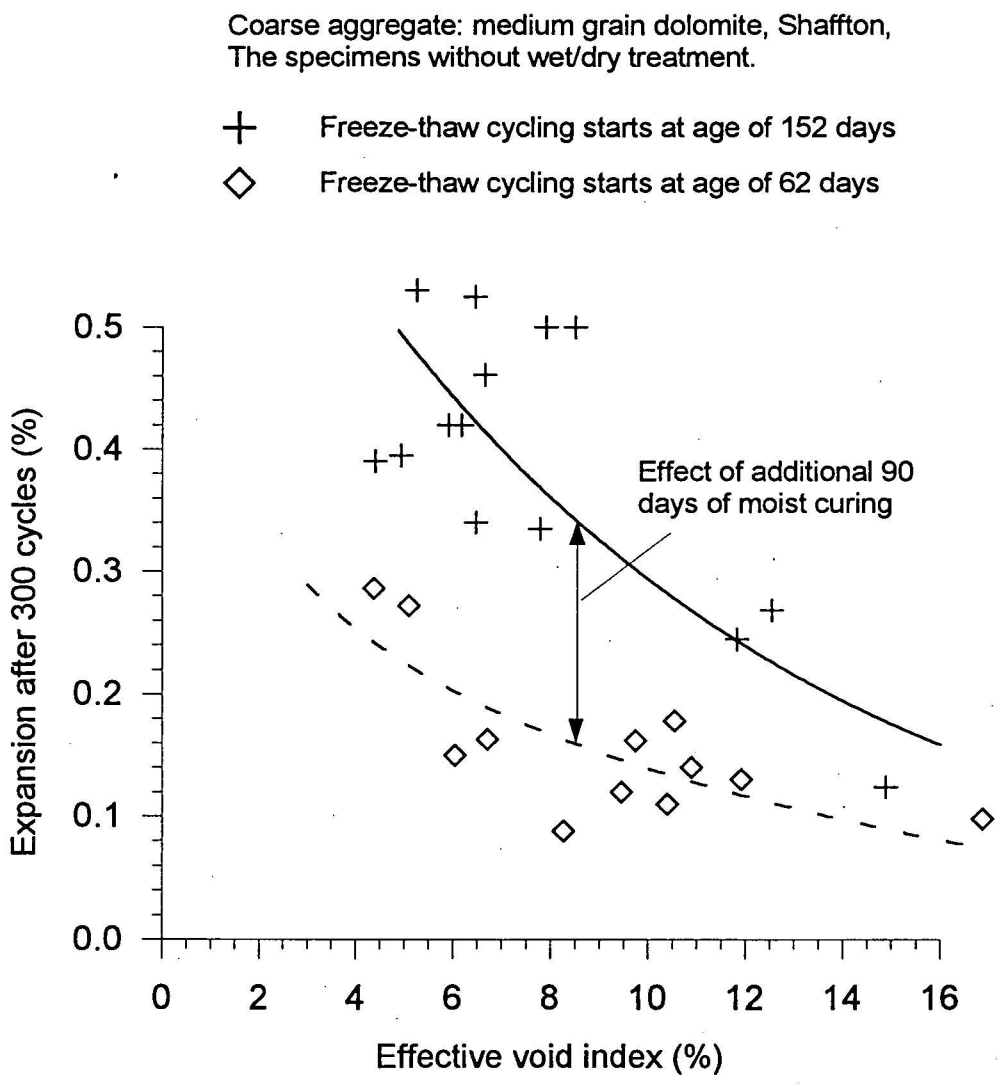

Fig. 4 Influence of period of moist curing on freeze-thaw response (coarse aggregate: Shaffton)

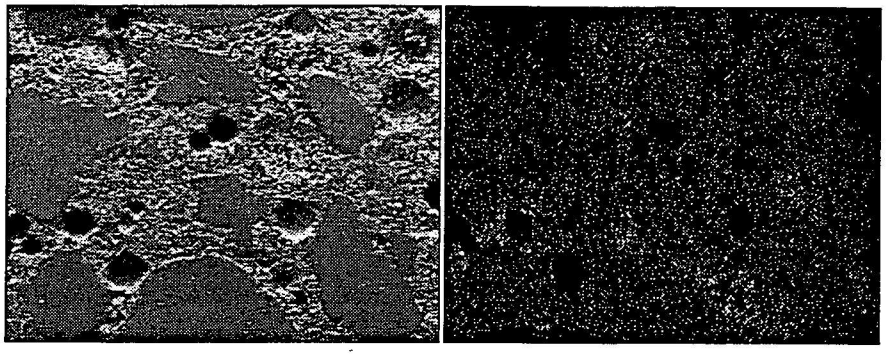

(a) Without wet/dry treatment, age of 62 days

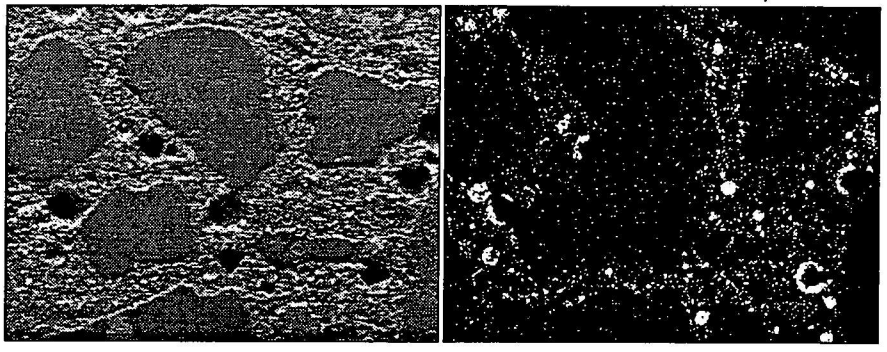

(b) With wet/dry treatment, age of 132 days

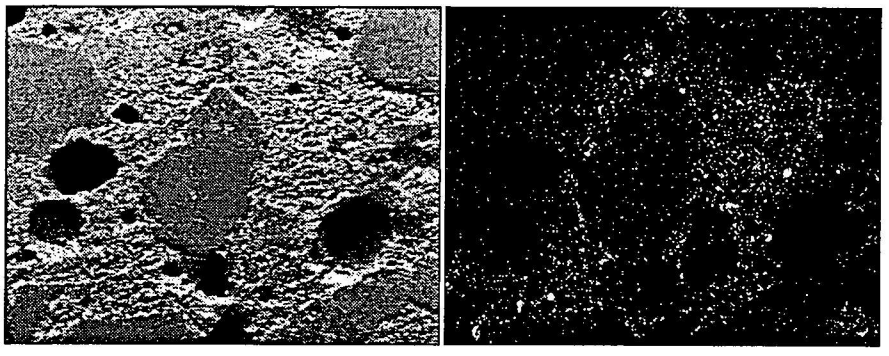

(c) Without wet/dry treatment, age of 152 days

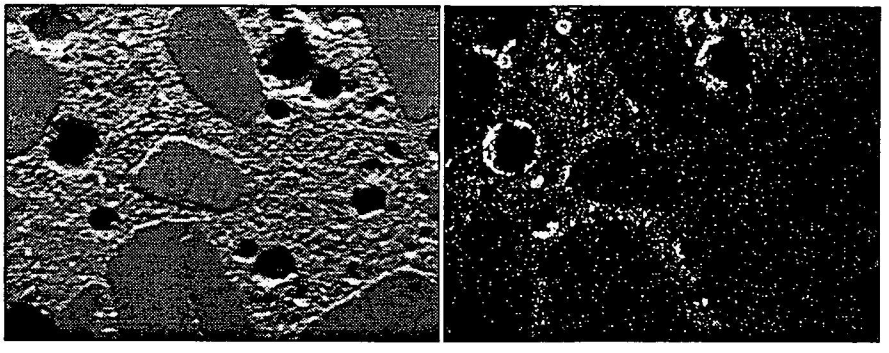

(d) With wet/dry treatment, age of 223 days

Fig. 5. SEM photomicrographs and corresponding sulfur maps for the mix using Cement 5, Fly ash 2, Conchem 25DP water reducer and Shaffton aggregate

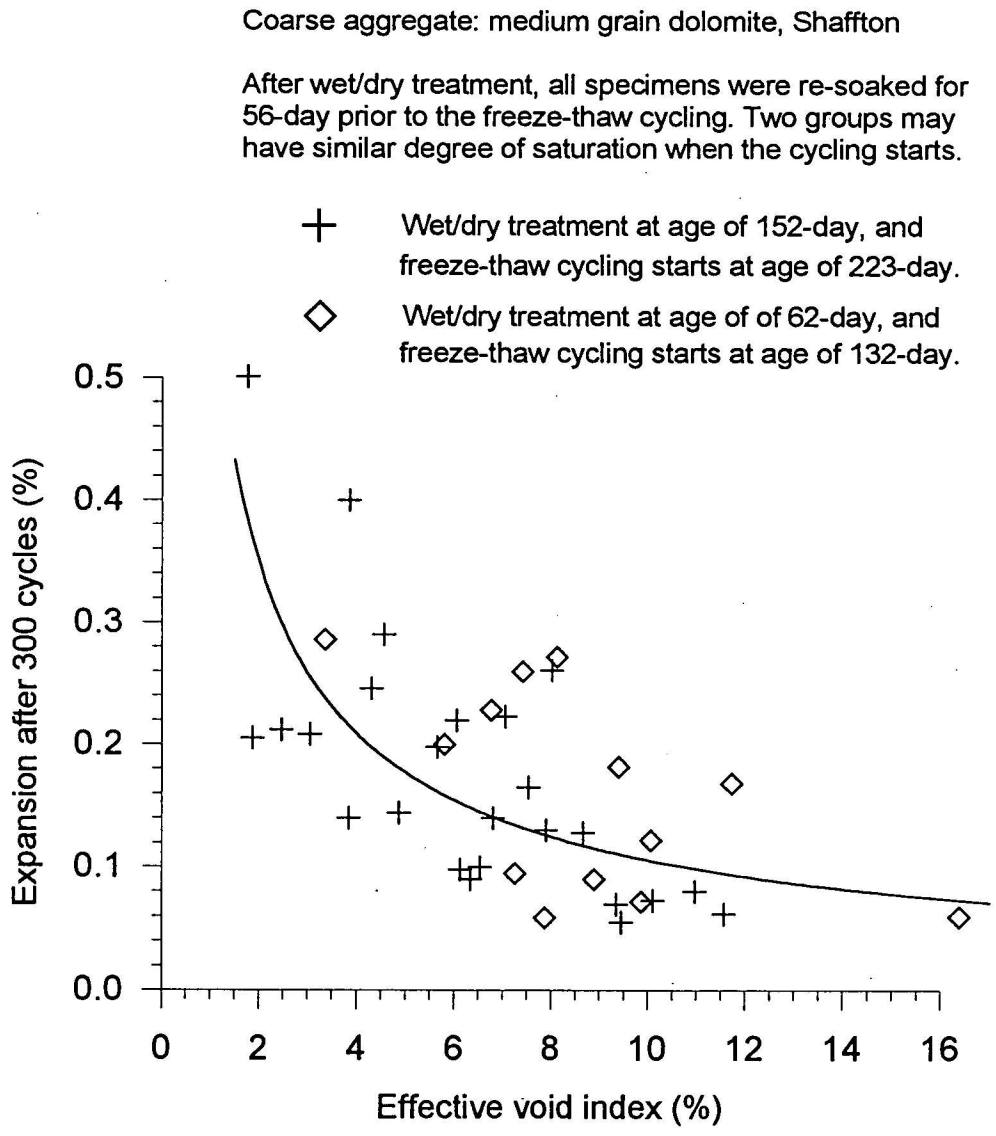

Fig. 6 Influence of effective void index on freeze-thaw response (coarse aggregate: Shaffton)

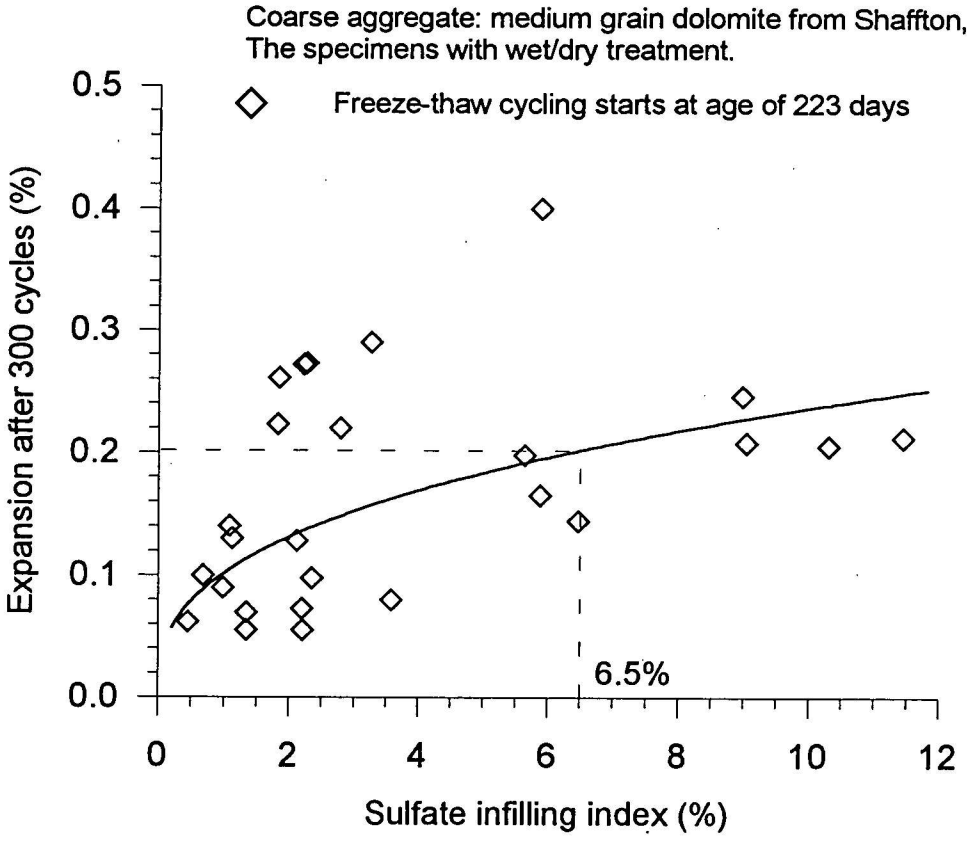

Fig. 7 Influence of ettringite infilling on freeze-thaw response (coarse aggregate: Shaffton)

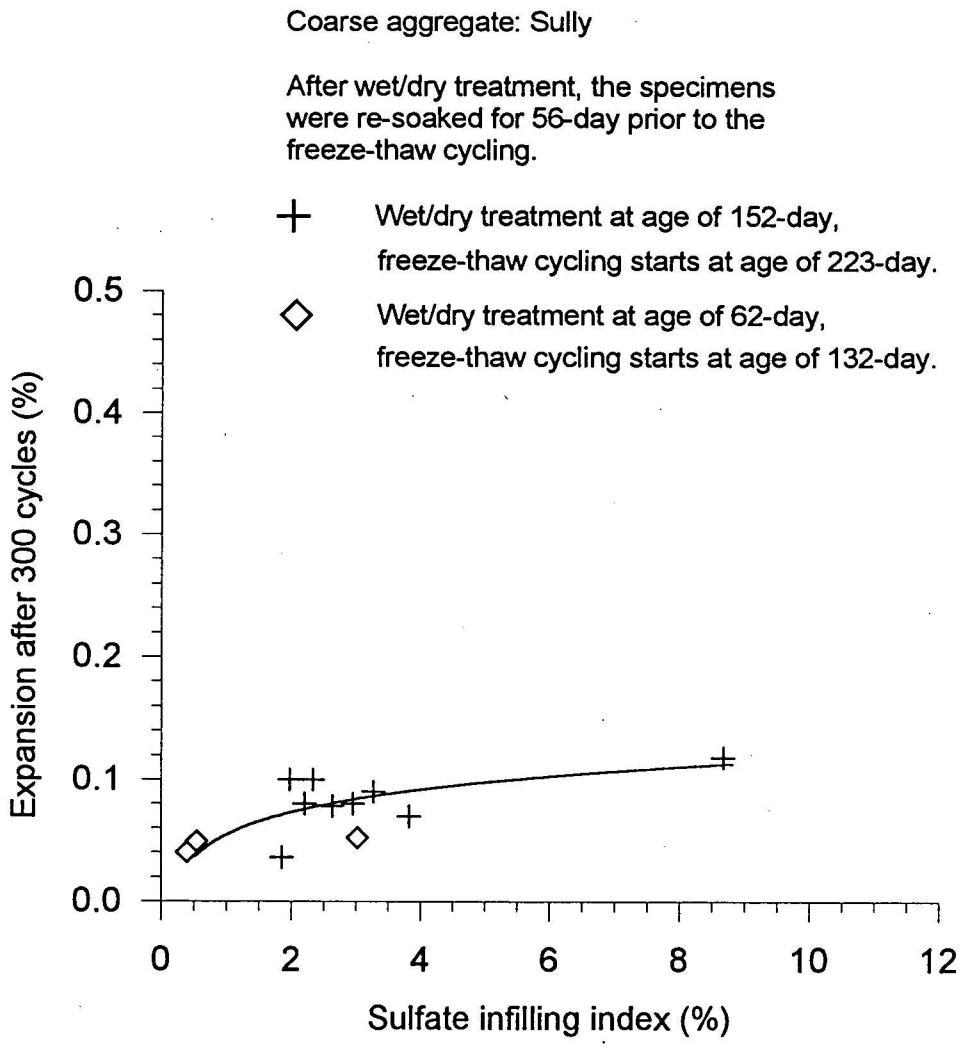

Fig. 8 Influence of ettringite infilling on freeze-thaw response (coarse aggregate: Sully)

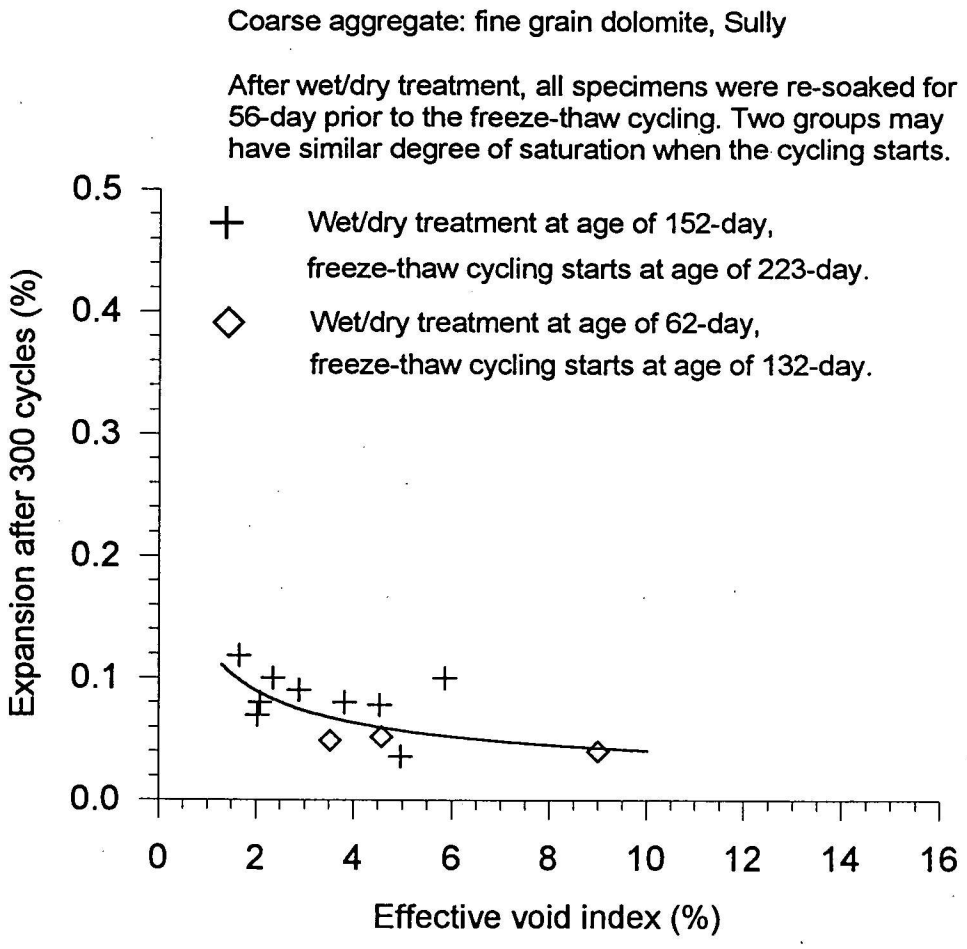

Fig. 9 Influence of effective void index on freeze-thaw response (coarse aggregate: Sully)

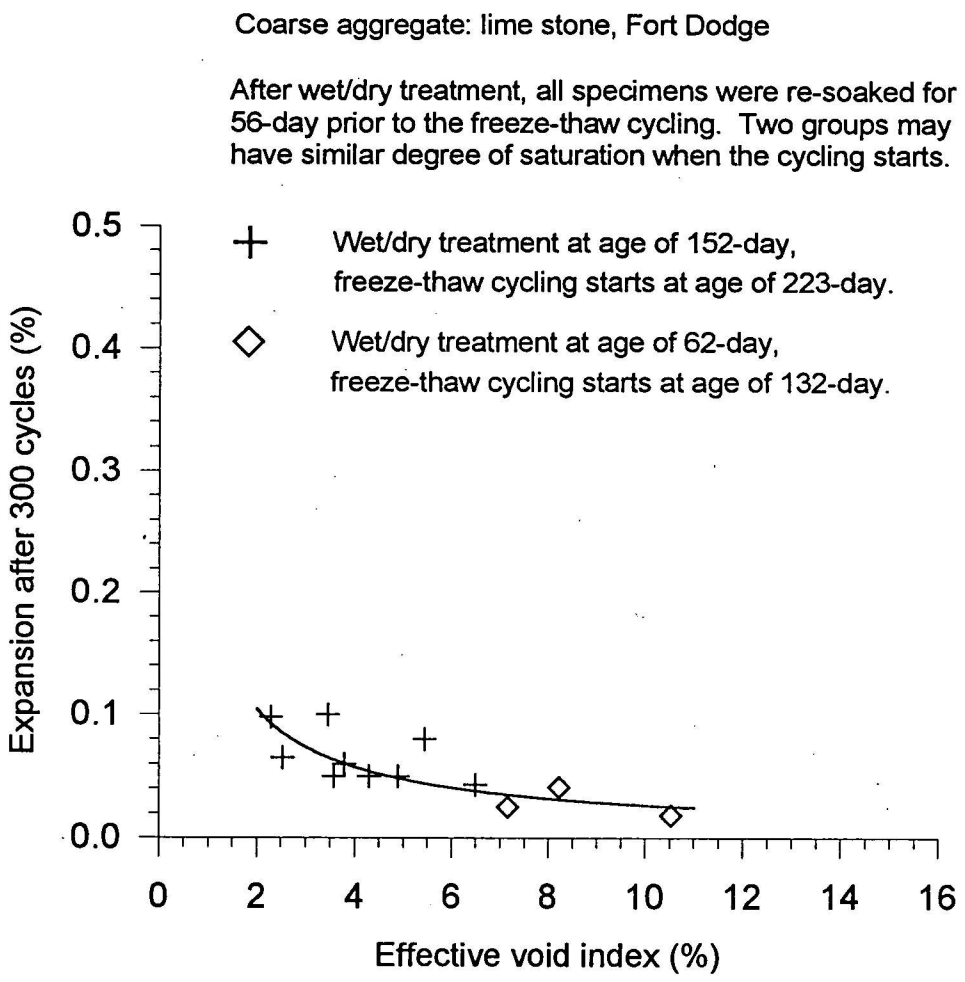

Fig. 10 Influence of effective void index on freeze-thaw response (coarse aggregate: Fort Dodge)

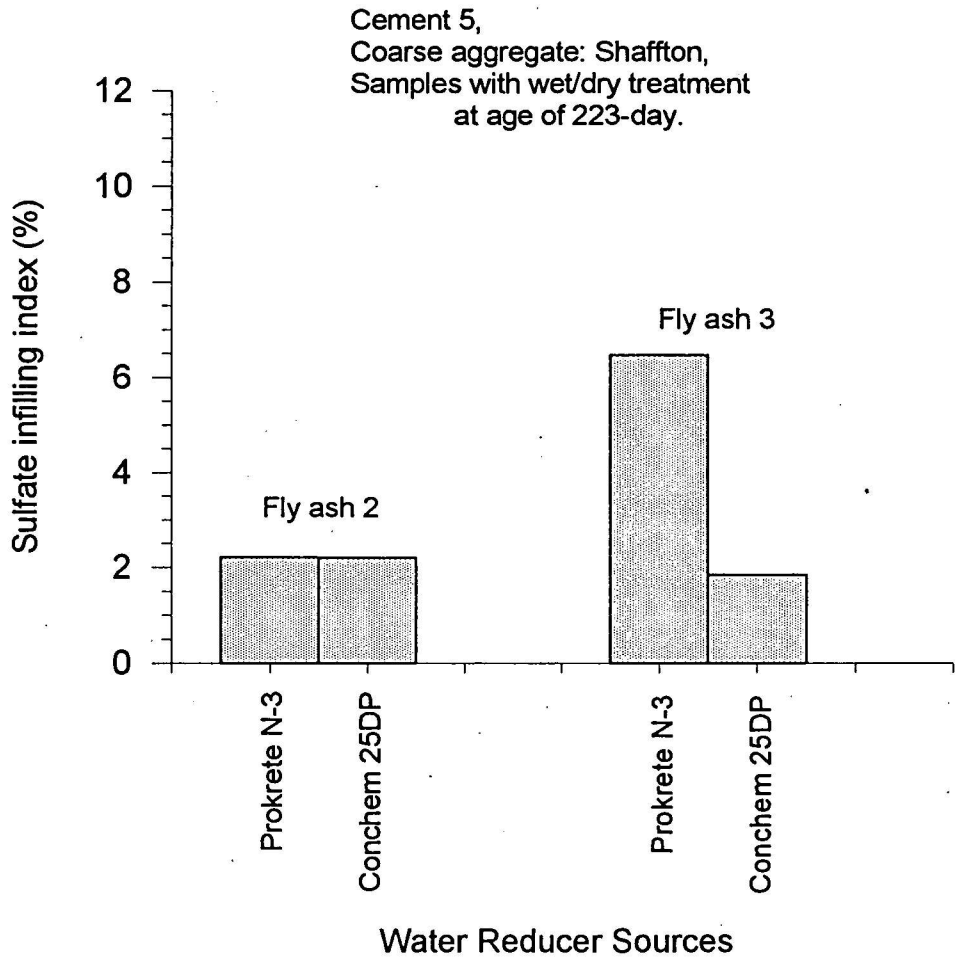

Fig. 11a Influence of type of water reducer on ettringite infilling (mixes using cement 5)

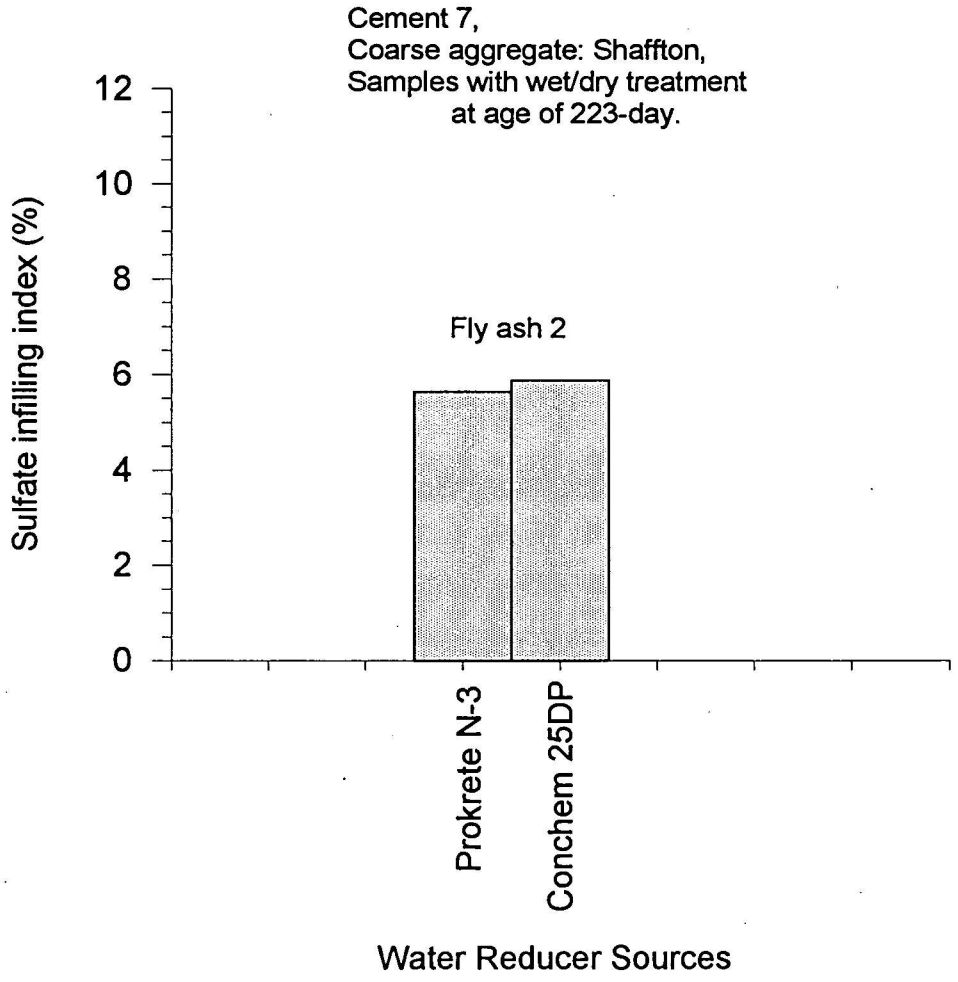

Fig. 11b Influence of type of water reducer on ettringite infilling (mixes using cement 7)

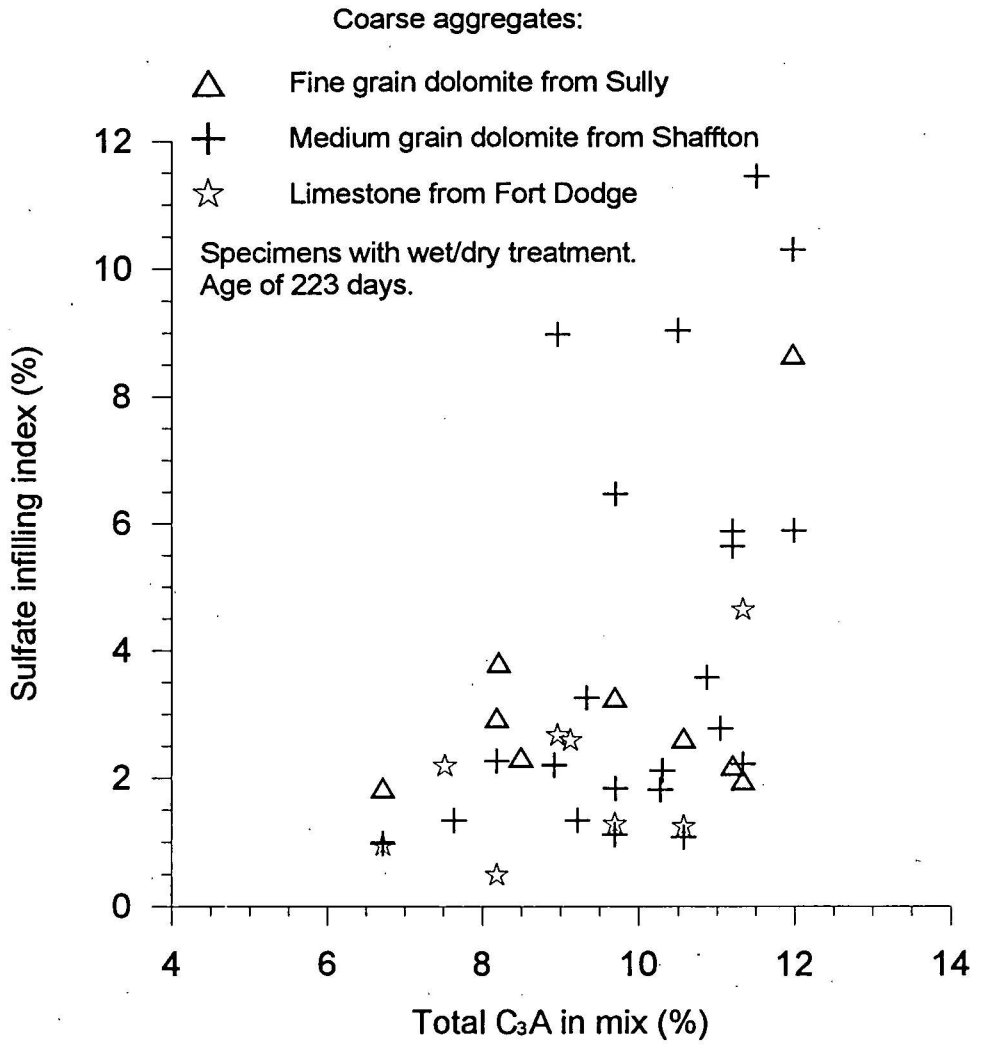

Fig. 12 Effect of total tricalcium aluminate in mix on ettringite infilling (specimens with wet/dry treatment and age of 223 days)

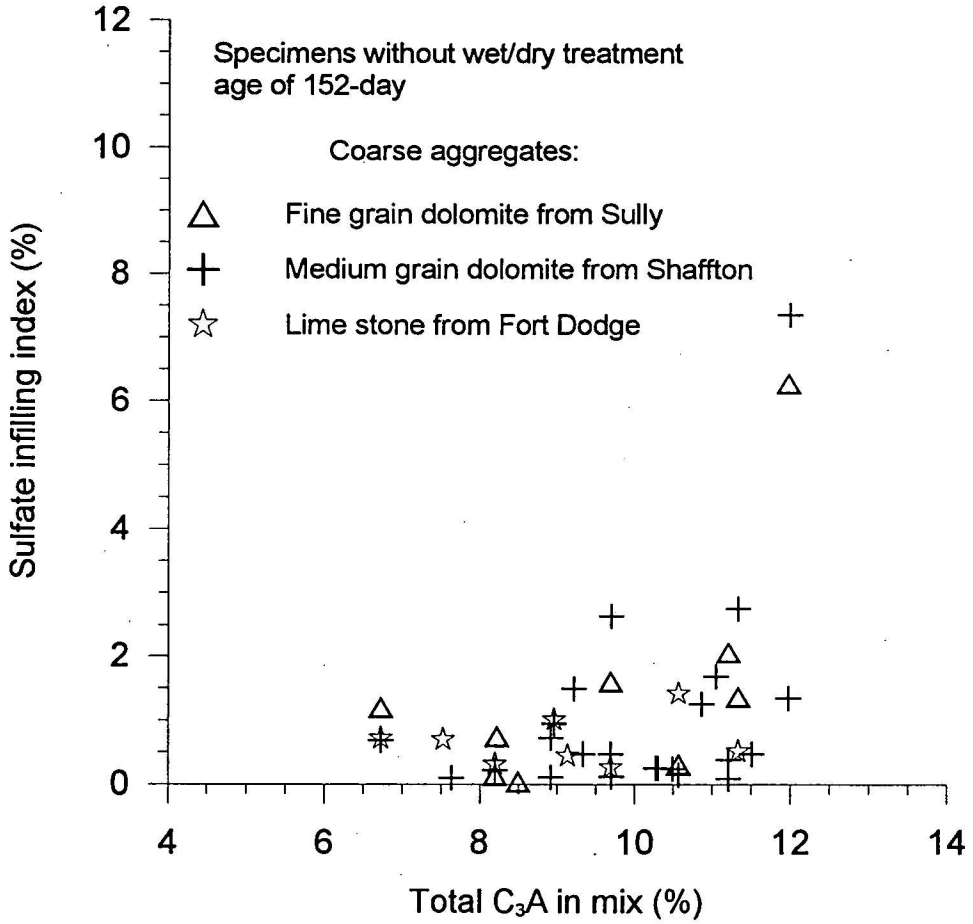

Fig. 13 Effect of total tricalcium aluminate on ettringite infilling (specimens without wet/dry treatment and age of 152 days)

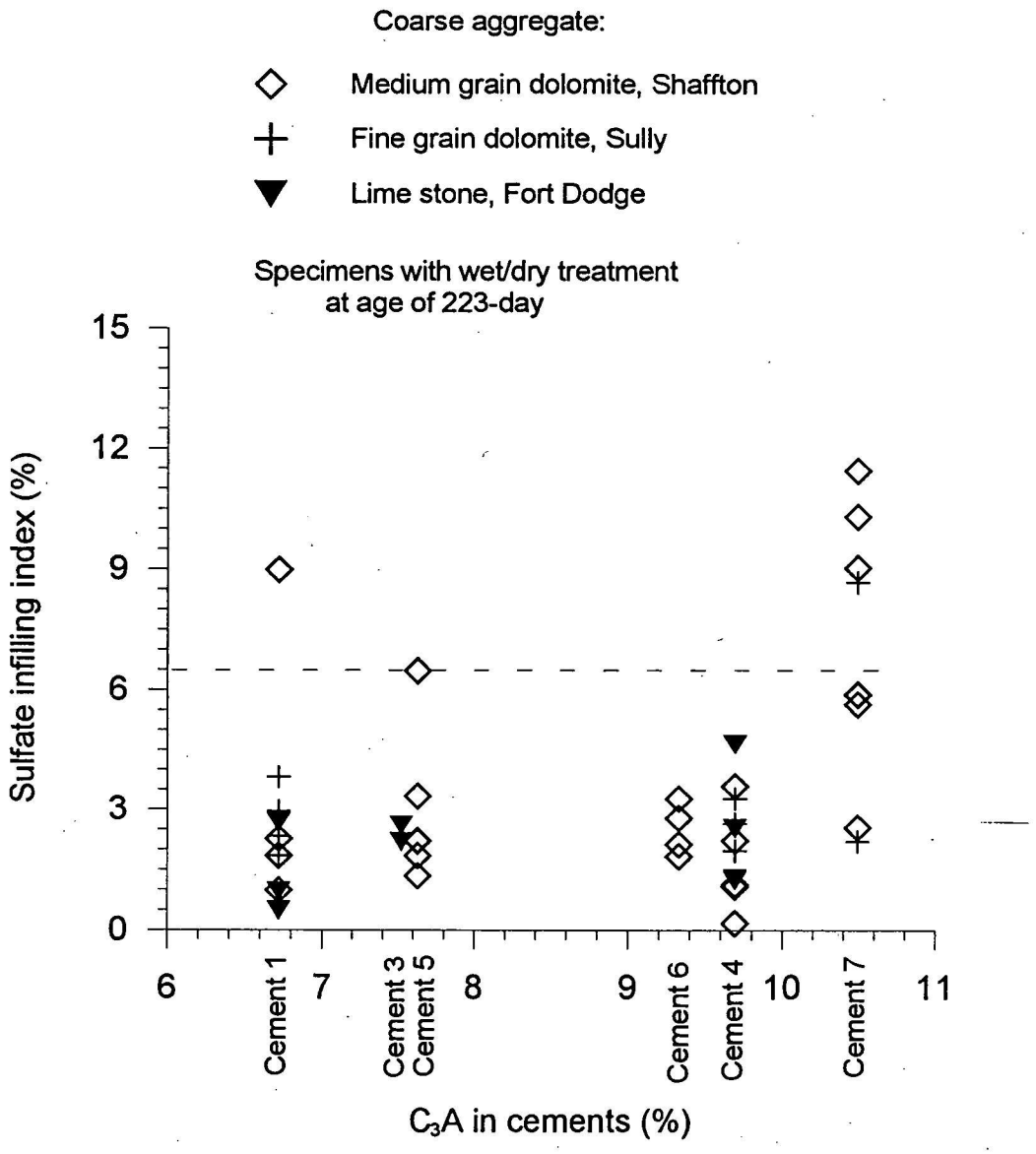

Fig. 14 Amounts of sulfate infilling for different types of cements

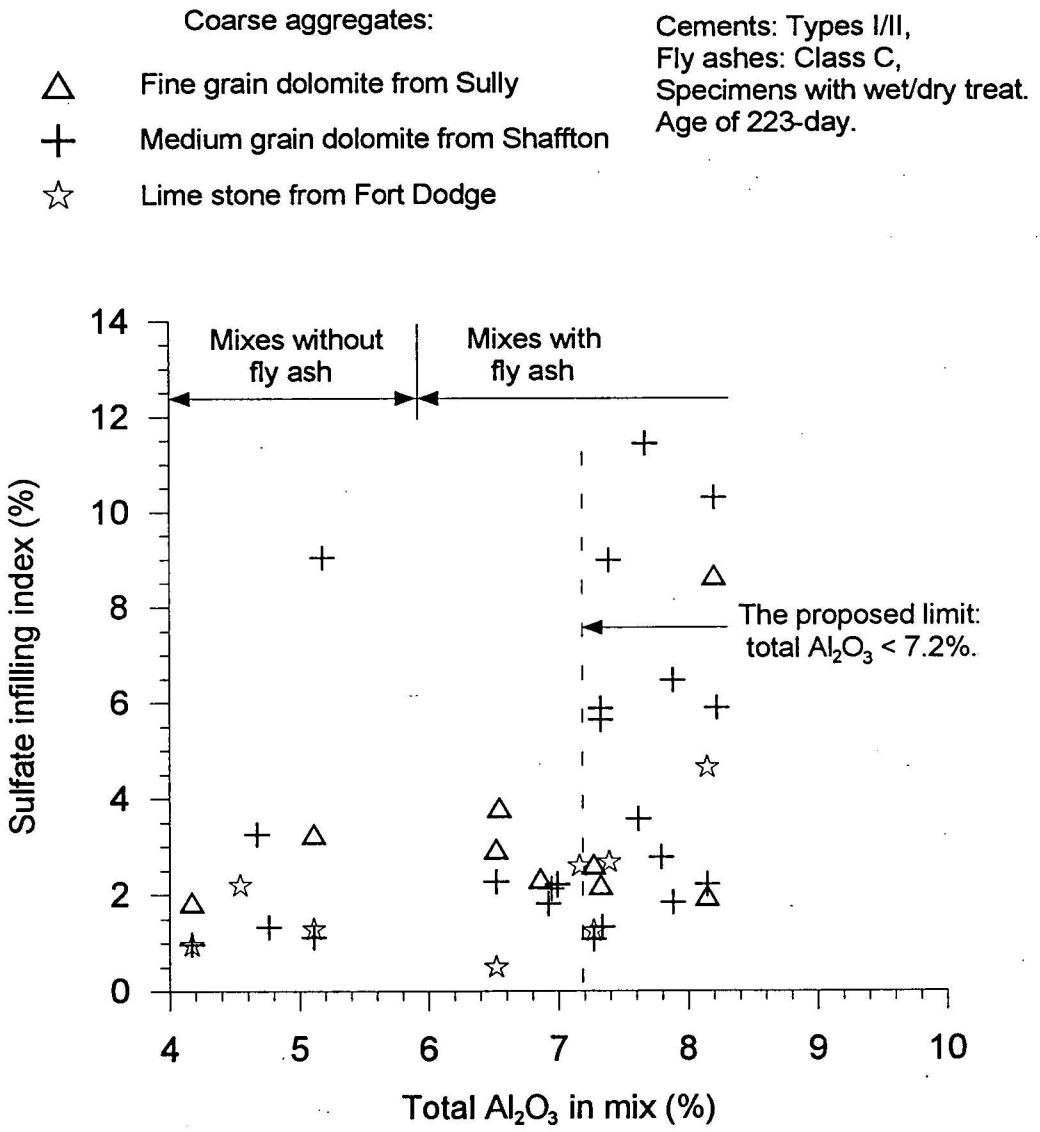

Fig. 15 Effect of total alumina in mix on ettringite infilling

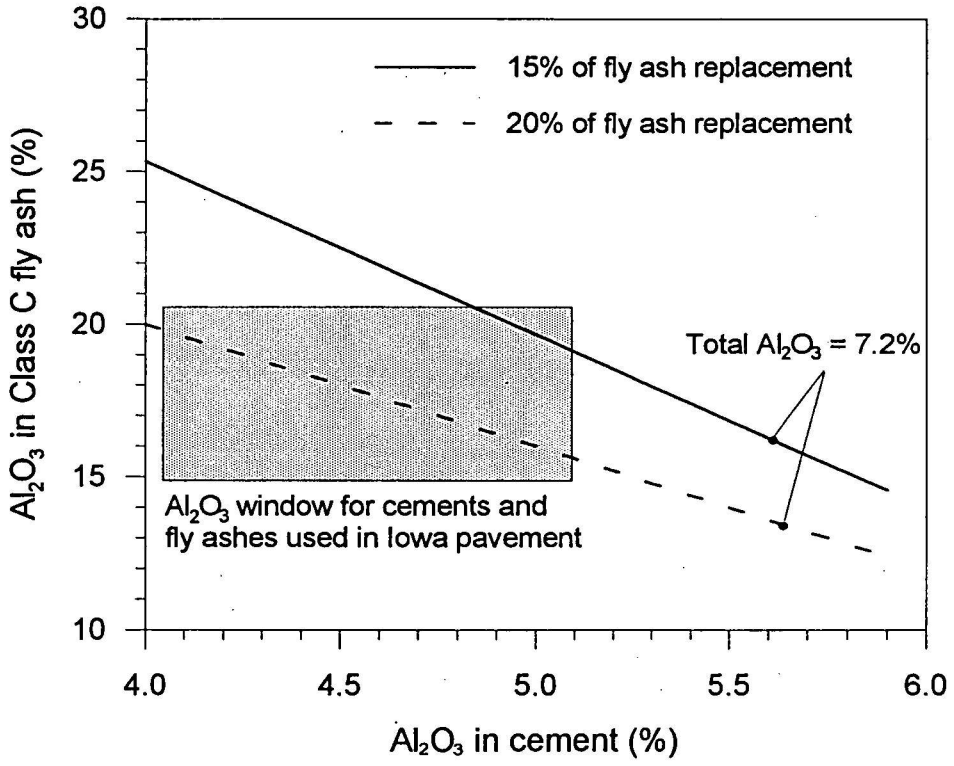

Fig. 16 Illustration of proposed limit on total Al_2O_3 in mix

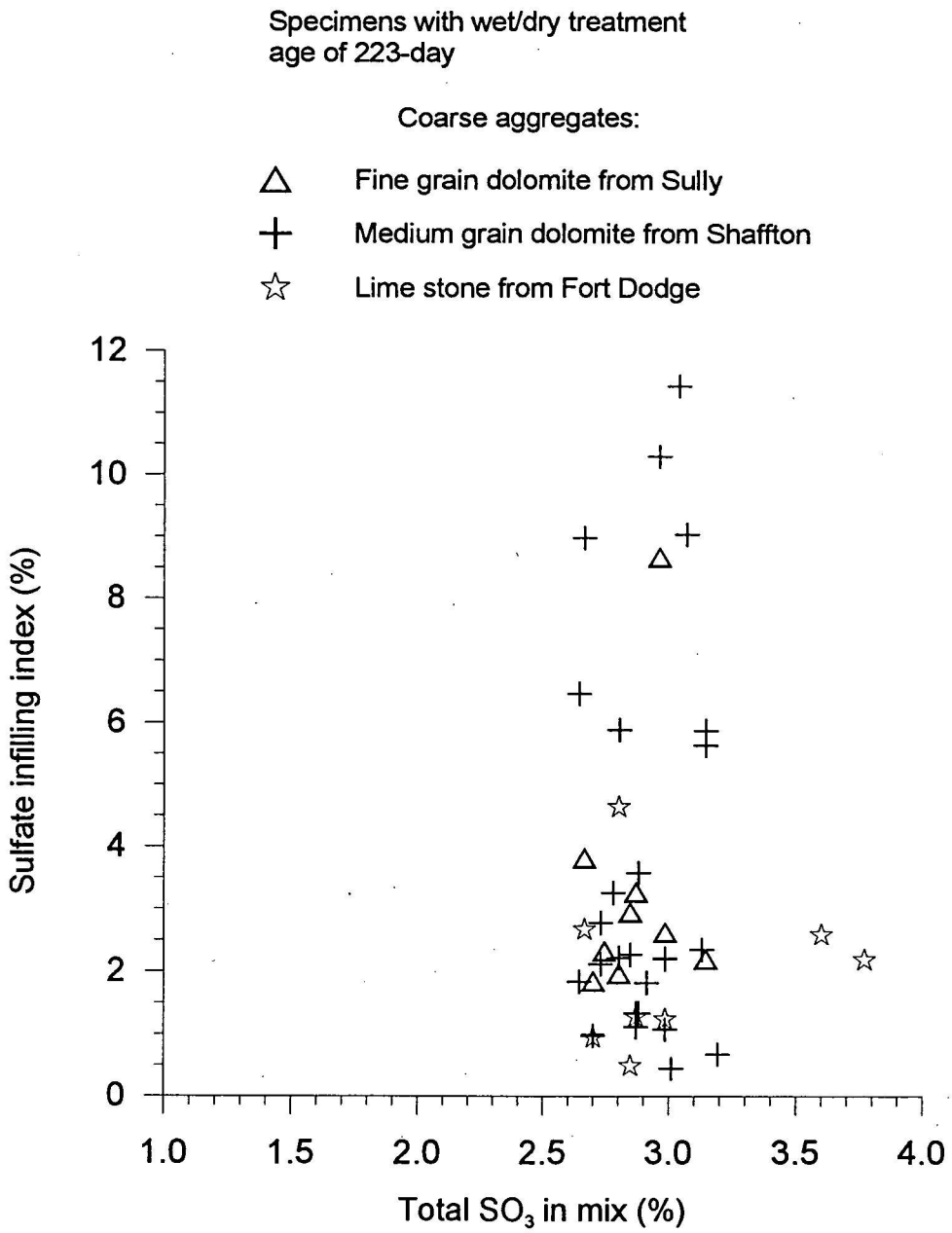

Fig. 17 Effect of total SO_3 in mix on ettringite infilling

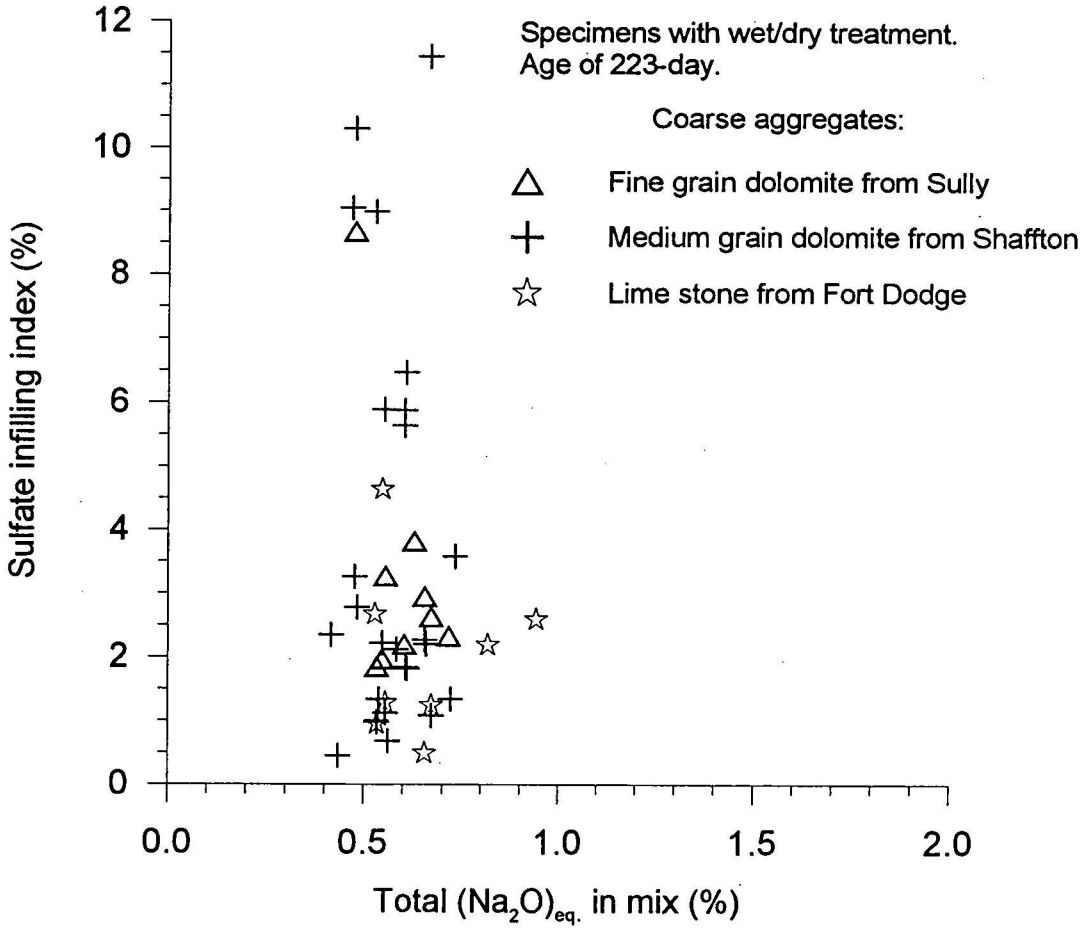

Fig. 18 Effect of total equivalent alkali on ettringite infilling

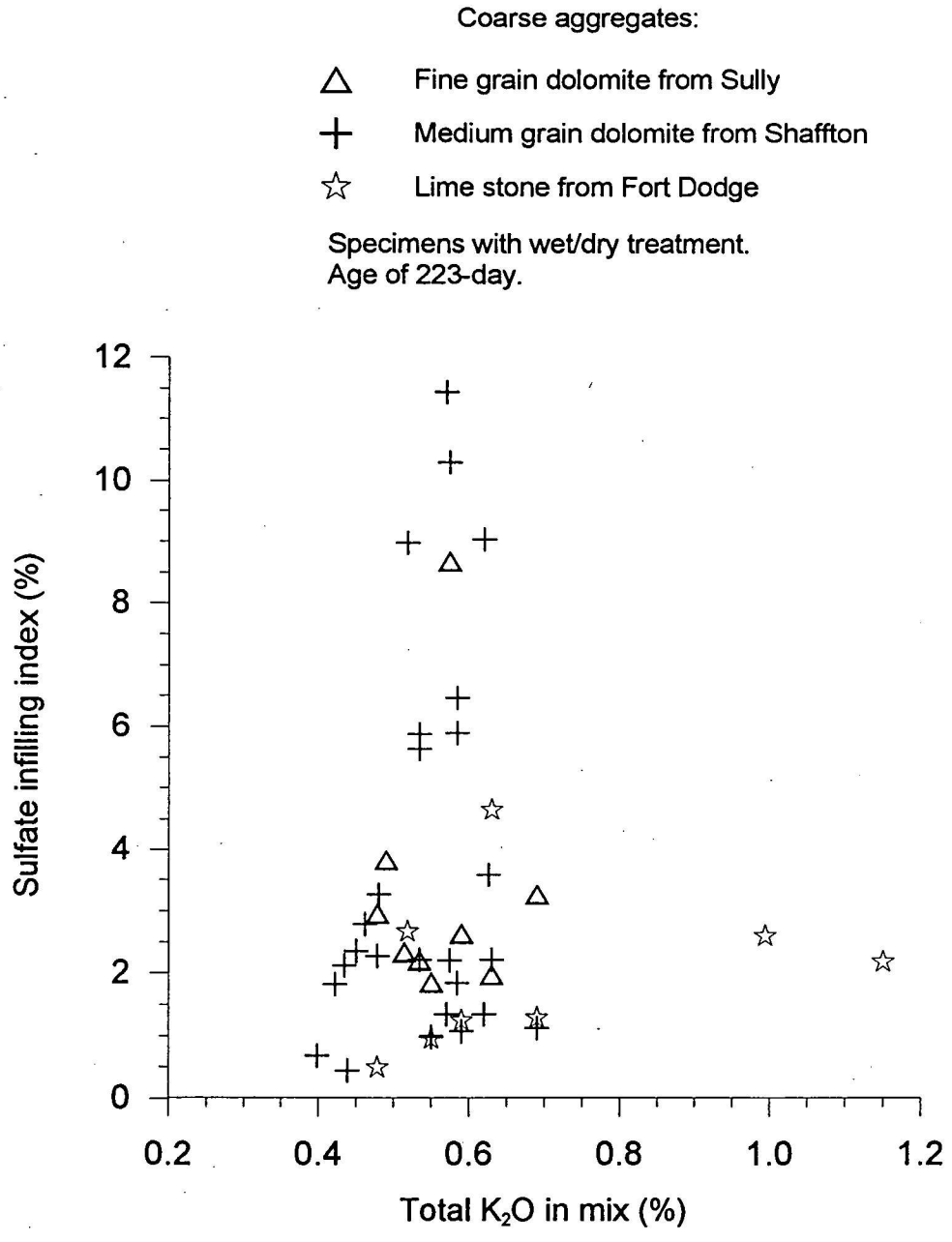

Fig. 19 Effect of total potassium alkali in mix on ettringite infilling

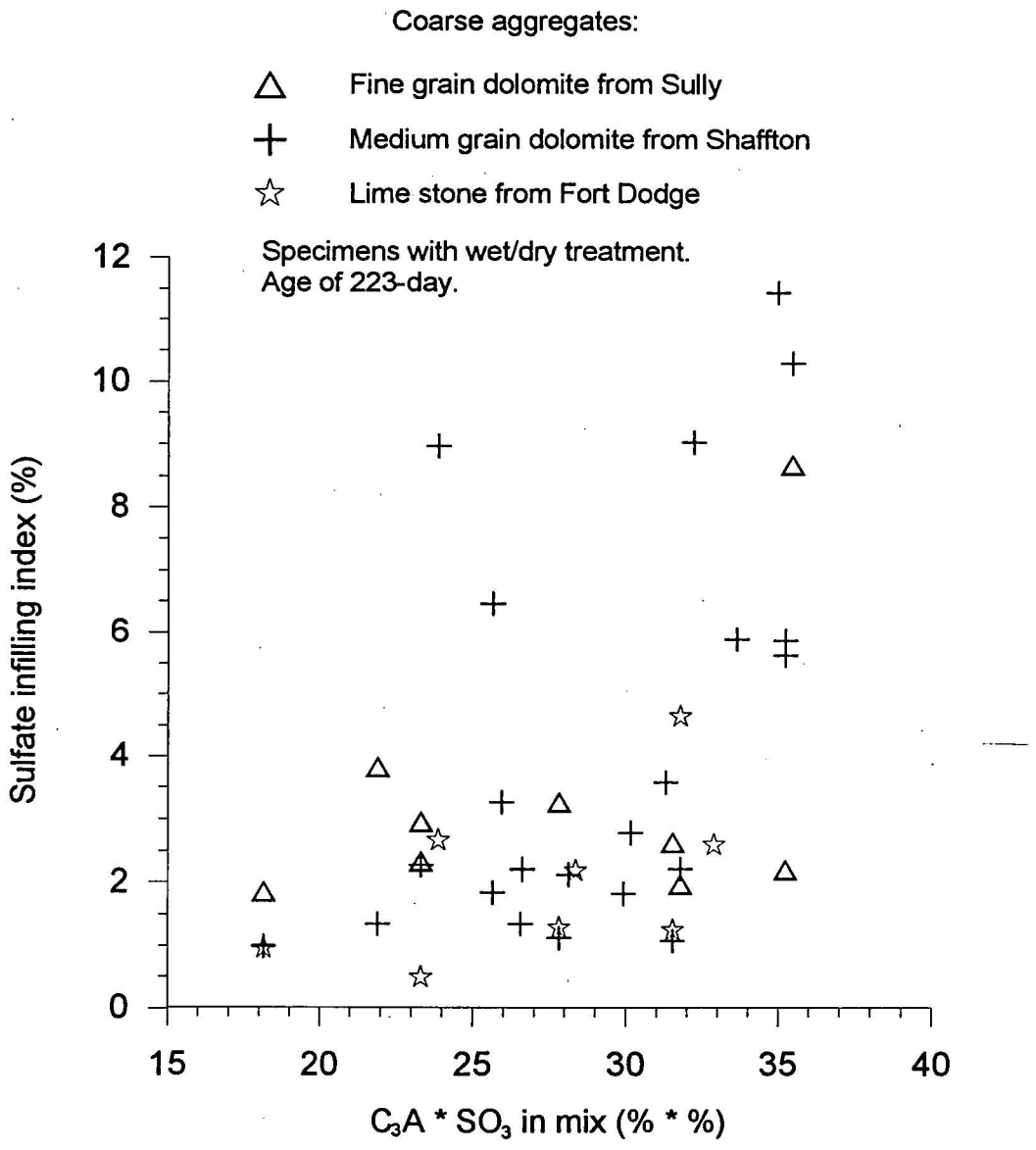

Fig. 20 Effect of C_3A*SO_3 in mix on ettringite infilling

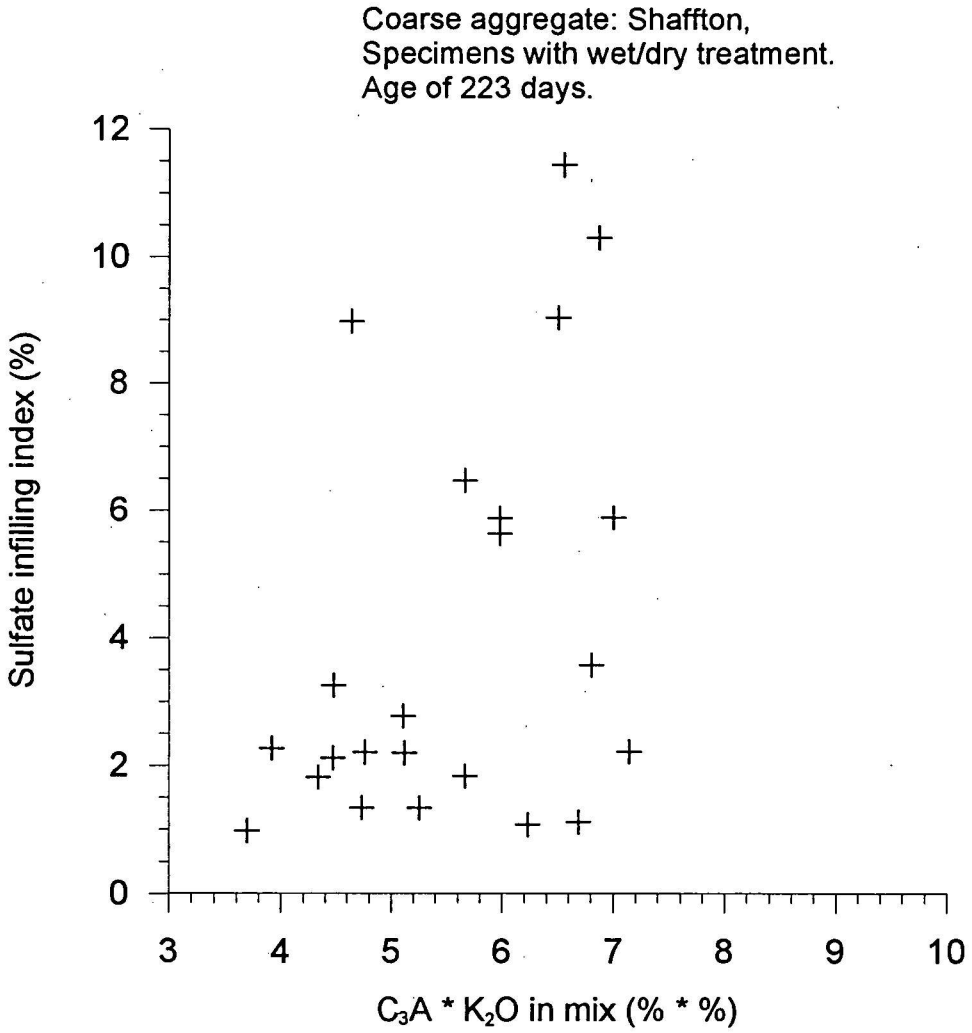

Fig. 21a Effect of C_3A*K_2O in mix on ettringite infilling (Shaffton coarse aggregate)

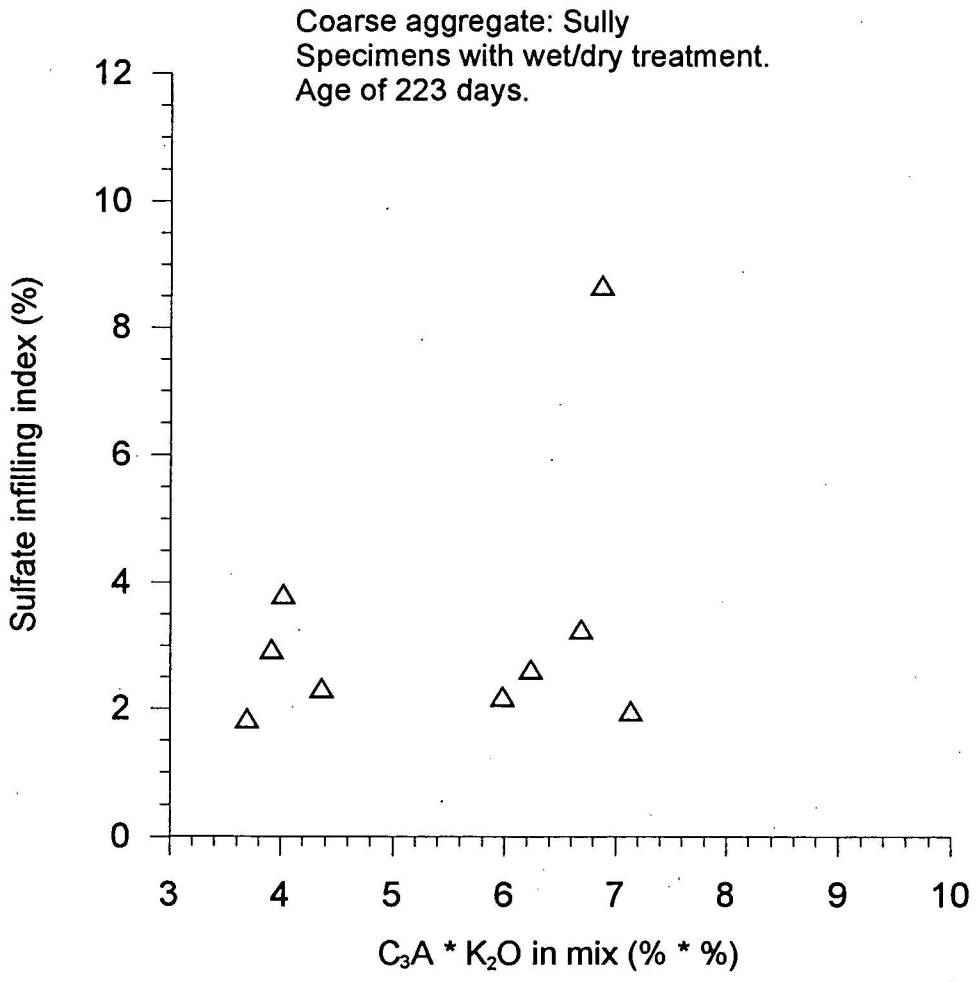

Fig. 21b Effect of C_3A*K_2O in mix on ettringite infilling (Sully coarse aggregate)

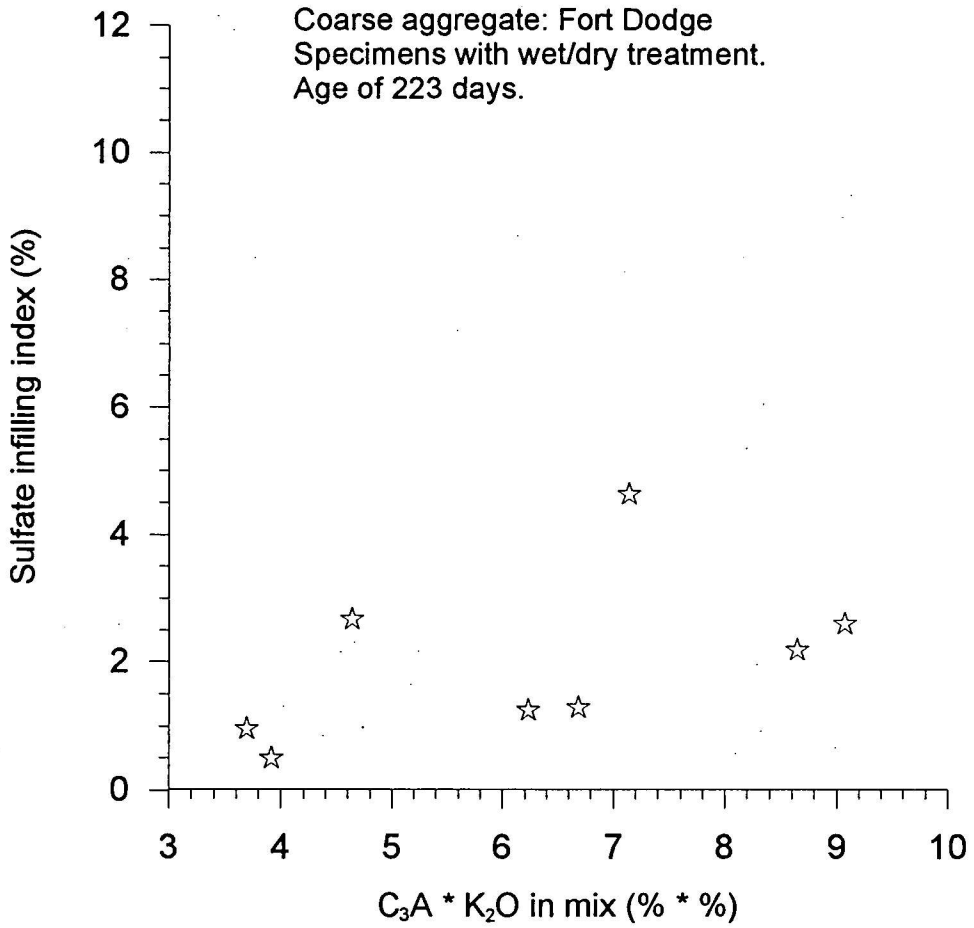

Fig. 21c Effect of C_3A*K_2O in mix on ettringite infilling
(Fort Dodge coarse aggregate)

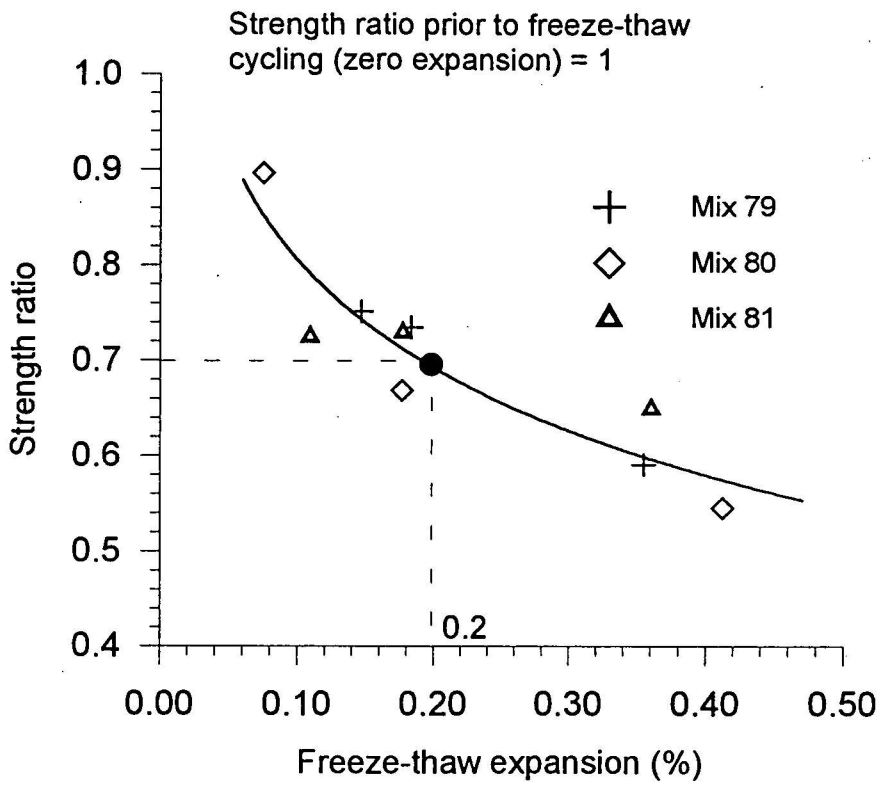

Fig. 22 Relationship between expansion and strength ratio